Catena 214 (2022) 106292

Contents lists available at ScienceDirect

Catena

journal homepage: www.elsevier.com/locate/catena

Climatic control on the Holocene hydrology of a playa-lake system in the western Mediterranean

Antonio García-Alix [a,b,*], Gonzalo Jiménez-Moreno [a], Fernando Gázquez [c,d], Ricardo Monedero-Contreras [b], Alejandro López-Avilés [a], Francisco J. Jiménez-Espejo [b,e], Miguel Rodríguez-Rodríguez [f], Jon Camuera [g], María José Ramos-Román [g], R. Scott Anderson [h]

[a] Department of Stratigraphy and Paleontology, University of Granada, Granada, Spain
[b] Instituto Andaluz de Ciencias de la Tierra (IACT), CISC-UGR, Armilla, Spain
[c] Water Resources and Environmental Geology Research Group, Department of Biology and Geology. University of Almería, Almeria, Spain
[d] Andalusian Centre for the Monitoring and Assessment of Global Change (CAESCG), University of Almería, Spain
[e] Biogeochemistry Program, JAMSTEC, Yokosuka, Japan
[f] Department of Physical, Chemical and Natural Systems, University Pablo de Olavide, Seville, Spain
[g] Department of Geosciences and Geography, Faculty of Science, University of Helsinki, Helsinki, Finland
[h] School of Earth and Sustainability, Northern Arizona University, Flagstaff, AZ, USA

ARTICLE INFO

Keywords:
Paleohydrological evolution
Southwestern Iberian Peninsula
Saline lakes
Aridification

ABSTRACT

Evaporitic lakes such as playa-lakes are characteristic of many arid regions and are unique environments with respect to fauna and flora, while being very vulnerable to climate and environmental fluctuations and threatened by the current global change scenario. Water balance oscillations in these systems can trigger the precipitation or dissolution of different evaporitic minerals, negatively impacting local biodiversity and economic activities. Here, we study the sedimentary record of a small saline pond from a playa-lake complex in southwestern Iberia in order to reconstruct the paleohydrological evolution of this area and assess potential anthropogenic disturbances. The different proxies studied in the ~11.9 ky old sedimentary record of the Laguna de la Ballestera suggest that the greatest lake extension and the highest water levels occurred during the Early Holocene, pointing to the wettest period of the record. Climate transitioned towards more arid conditions during the Middle Holocene, and even more dramatically during the Late Holocene. In this last stage the wetland surface and the water level largely diminished and gypsum precipitation gradually increased pointing towards a negative precipitation/evapotranspiration balance and lowest water levels. Summer desiccation likely occurred under this scenario, especially after ~1.0–0.9 cal ky BP coeval with the Medieval Climate Anomaly, when gypsum content started to rise abruptly. However, this significant gypsum precipitation was only associated with a massive drop in the siliciclastic content and scarce carbonates (dolomite and calcite) during the last ~400 years. This evidence suggests a shift from a (semi) permanent to a temporal/seasonal hydrological regime. The environmental evolution of this wetland responded to the general climatic evolution of the western Mediterranean during the Holocene, being mostly controlled by changes in insolation. Our data also show that the environmental response of the studied wetland to natural climate variations was only significantly disturbed by human activities since the 20th century, especially in the second half of the century, deduced by abrupt fluctuations in the siliciclastic, gypsum and organic content in the sediments, as well as by the enhanced sedimentary accumulation rates, probably as a response to changes in the hydroperiod of the lake and in the catchment land use.

1. Introduction

The current scenario of global change is boosting the expansion of drylands – arid, semi-arid and dry sub-humid areas – in mid-low latitudes and accelerating desertification processes (IPCC, 2019). Drylands cover almost 34 % of surface in the European countries of the Mediterranean fringe and in the case of Spain they represent 69 % of the total land surface (Maréchal et al., 2008; IPCC, 2019). The recent

* Corresponding author Department of Stratigraphy and Paleontology, University of Granada, Granada, Spain.
E-mail address: agalix@ugr.es (A. García-Alix).

https://doi.org/10.1016/j.catena.2022.106292
Received 14 October 2021; Received in revised form 17 February 2022; Accepted 6 April 2022
Available online 13 April 2022

climate change is also amplifying salinization and sodification processes in drylands, particularly, where evaporite deposits occur (Maréchal et al., 2008). This phenomenon affects 1–3 million hectares in Europe, especially in the southwestern area, and these figures have risen during recent decades (Maréchal et al., 2008). In this regard, the dual effect of aridification-desertification and soil salinization-sodification has turned a major environmental problem in southern Iberia, which is the most severely-affected region in Europe by these processes due to its climatic and geological features (Rodríguez-Rodríguez, 2007; Toth et al., 2008; Rodríguez-Rodríguez et al., 2010; IPCC, 2019). These phenomena also have a significant impact on the economic activities of this area, mainly agriculture and livestock production, that have been adapted for these kinds of conditions, enhancing cultivation of dry-adapted species, or using intensive irrigation (Rodríguez-Rodríguez, 2007; Beltran et al., 2012). However, it is not completely known to what extent the environmental degradation of this area has been either caused or amplified by human activities. Marked anthropogenic impacts on southern Iberian environments, related to agricultural and mining activities, are recognized among the earliest ones in westernmost Europe, dating back to, at least, 4.2 cal ky BP (Carrión et al., 2007; López-Sáez et al., 2018). Nevertheless, recent studies on climate-sensitive records from shallow endorheic saline lakes in southwestern Iberia challenged the interpretation of such anthropogenic anomalies, and associated these environmental changes to fluctuations in precipitation patterns rather to human influence (e.g., Medina Lake; Schröder et al., 2020). These new findings suggest that the extent of paleoenvironmental human impacts in southwestern Europe is still a matter of discussion.

Large playa-lake complexes, such as those developed in the Guadalquivir River Basin, are one of the evaporite systems in southern Iberia more affected by environmental and human threats, and their

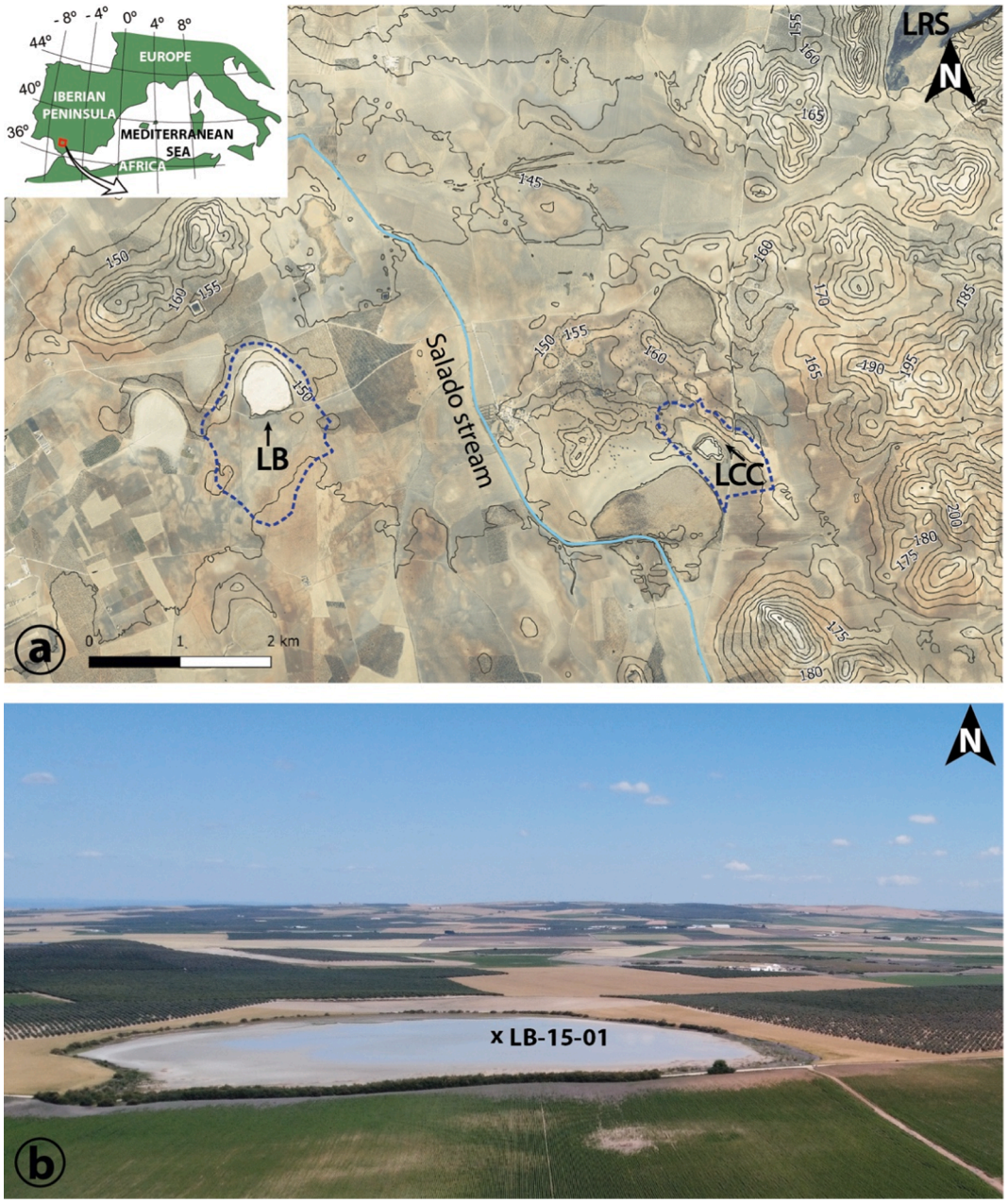

Fig. 1. Location of the Laguna de la Ballestera (LB) in southern Iberian Peninsula. **a)** Regional situation of the LB along with other playa-lakes mentioned in the text: Laguna del Calderón Chica (LCC) and Laguna de Ruíz Sánchez (LRS). The catchment basins of LB and LCC are marked with dashed lines. **b)** Aerial picture of the LB playa-lake in May 2021. The LB-15–01 core was recovered in the depocenter of the LB playa-lake.

clastic–evaporite alternations are excellent archives of past hydrological regimes (e.g., Sinha et al., 2006; Valero-Garcés et al., 2000), since these sensitive environments can register both natural (e.g., changes in the watershed patterns due to differential uplifting, infilling, and/or evapotranspiration) and anthropogenic (e.g., water pumping, drainage, land-use changes, and/or pollution) pressures (Rodríguez-Rodríguez, 2007; Rodríguez-Rodríguez et al., 2010). The understanding of past natural hydrological dynamics and potential human-induced disturbances is of paramount importance to apply the most precise conservation, management and remediation practices in these environmental-sensitive saline areas of southern Iberian Peninsula (Klinge et al., 2017; McFadden and McAuliffe, 1997). In this paper we study the Holocene evolution of the Laguna de la Ballestera (Fig. 1), a (almost) non-anthropogenically modified playa-lake in the Guadalquivir River Basin (southwestern Spain), whose Holocene sedimentary record can shed light on the past hydrology of evaporite environments in this environmentally vulnerable region.

1.1. Regional setting

The Laguna de la Ballestera (LB) (37°22′5.07″ N, 5°10′37.40″ W, and 150 m a.s.l.), located in the Guadalquivir River Basin near the Osuna town, is a 25.5-ha temporal playa-lake with a pseudo-circular shape and a watershed of 145.2 ha (Rodríguez-Rodríguez et al., 2010) (Fig. 1). It is one of the nine water bodies that constitute the endorheic complex of La Lantejuela (Seville, southern Iberia), a Natural Reserve since 1989 (Moreira Madueño, 2005) and included in the Andalusian Wetland Plan from the Environmental Council of Andalusia (Montes et al., 2004). Most of the water bodies in this playa-lake complex have been anthropogenically modified and desiccated for agricultural purposes. In most of the cases the drainage activities were successful, but salinity in the soil remained very high and the production yields were low in the area. Consequently, these basins were abandoned for agriculture. Currently, such still drained playa-lakes have an ephemeral hydroperiod (Beltrán et al., 2012). These anthropogenic impacts have been insignificant in the LB and Laguna Calderón Chica (LCC) playa-lakes, most probably due to unsuccessful past experiences in other basins with extremely high salinity of water and soils. Therefore, both basins remained undrained until present and La Lantejuela playa-lake complex was finally protected as Natural Reserve in the last decade of the 20th century (Rodriguez-Rodriguez and Schilling, 2014) (Fig. 1).

La Lantejuela playa-lake complex is located on Neogene and Quaternary alluvial materials, which constitute the unconfined Osuna-La Lantejuela (O-LL) aquifer, overlying Triassic evaporitic sediments of the Keuper lithostratigraphic unit. The origin of the basin hosting the O-LL aquifer is probably related to tectonic processes that affected the basement during the Upper Miocene, forming a depression that was filled up with alluvial materials in a palustrine environment. The subsequent formation and origin of the playa-lake complex was due to several factors, including diapirism, karstification of the Keuper evaporites and aeolian deflation (Rodríguez-Rodríguez et al., 2008; Moral Martos, 2016). The Triassic evaporitic sediments along with the high evaporation from the surface of the playa-lakes generate high salinity of the groundwater, ranging from <2 mS/cm to more than 15 mS/cm near the playa-lakes. In fact, groundwater in the O-LL aquifer exhibits a geochemical evolution of increasing concentrations of Na and Cl from the edges of their watersheds towards the position of the playa-lakes (Rodríguez-Rodríguez et al., 2008). These playa-lakes are usually dry for more than 6 months every year. The normal hydroperiod spans from January to the end of June and the maximum water level (~25 cm in the case of LB) is generally reached in February and March (Rodríguez-Rodríguez, 2007).

The annual precipitation in this area is slightly higher than 500 mm and the mean annual temperatures are ~18–19 °C, being one of the hottest areas in Spain. From June to September mean temperatures are usually higher than 25 °C, and precipitation is ~50 mm (Spanish National Weather Agency - AEMet Open Data, 2021). The hydric balance of these playa-lakes depends on the interannual variability between inputs (precipitation, runoff, or groundwater) and evapotranspiration (Rodríguez-Rodríguez, 2007). Surface runoff inputs in the LB represent around 50 % of the effective precipitation in the catchment since the other half infiltrates throughout the highly-permeable materials (sandy marls and conglomerates), recharging the O-LL aquifer. This local infiltration along with the precipitation onto the main recharge area of the O-LL aquifer represent the main water contribution -via groundwater- to the LB at present. Additionally, depending on the hydrological season, the water of the LB playa-lake can also recharge the aquifer (Rodríguez-Rodríguez et al., 2008).

1.2. Past and present hydroclimatic features in southern Iberia

The southern Iberian Peninsula, located between Atlantic, Mediterranean, low and high latitude atmospheric dynamics, is an especially sensitive and vulnerable area to present and past climate changes (Lionello et al., 2006;Trigo et al., 2006; Gimeno et al., 2010). These features make this area a key location for understanding climatic spatial patterns and their fluctuations across different timescales (Camuera et al., 2018; Schirrmacher et al., 2020; García-Alix et al., 2021). The North Atlantic Oscillation (NAO) controls winter precipitation in southern Iberia (Hurrell et al., 2013). Nevertheless, while southeastern Iberia can also be affected by Mediterranean dynamics and thus, by Mediterranean moisture sources during other seasons, Atlantic moisture is the main source of precipitation throughout the year in southwestern Iberian areas (Gimeno et al., 2010). Similar patterns have been observed from past sedimentary records in the Western Mediterranean area, pointing to a NAO control on rainfall dynamics, at least, since the Middle-Late Holocene (Fletcher et al., 2013; Toney et al., 2020). The Holocene hydroclimate in the entire western Mediterranean region overall shows a humid Early Holocene, a transitional Middle Holocene, with wetter conditions at the beginning and more arid conditions at the end of this period, and finally, a Late Holocene that depicts an aridification trend (e.g., Fletcher and Sánchez Goñi, 2008; Anderson et al., 2011; Jiménez-Moreno and Anderson, 2012; Martínez-Ruiz et al., 2015; Zielhofer et al., 2017; Ramos-Román et al., 2018; Toney et al., 2020; García-Alix et al., 2021). The seasonality and the precipitation source also seem to fluctuate throughout the Holocene in the western Mediterranean realm; while the Early-Middle Holocene mainly registered winter Atlantic-sourced precipitation, during the Middle-Late Holocene the seasonality of the precipitation slighty shifted towards more late winter-early spring precipitation with certain influence of Mediterranean moisture sources (Zielhofer et al., 2017; Toney et al., 2020; García-Alix et al., 2021). Vegetation responded to these paleohydrological changes in southern Iberia, and for example, the Mediterranean forest registered a maximum abundance during the Early Holocene that decreased from the Middle to the Late Holocene, while xeric herbs and grasses gradually expanded (e.g., Anderson et al., 2011; Ramos Román et al., 2018).

Most of the paleoenvironmental data from the western Mediterranean region comes from marine records (e.g., Martrat et al., 2004; Martrat et al., 2007; Moreno et al., 2005; Fletcher and Sánchez Goñi, 2008; Chabaud et al., 2014; Bahr et al., 2014; Martínez-Ruiz et al., 2015; Sierro et al., 2020, among others). Although these marine records can reflect some terrestrial environmental variables, they are challenging for reconstructing hydrological changes and environmental responses of past terrestrial environments, due to limited age resolution, bioturbation and bottom currents that affect proxy interpretation, among others (Bahr et al., 2014). Additionally, although marine records usually extend further in the past compared to lacustrine records (Lang and Wolff, 2011), it is difficult to obtain high-resolution archives of the last hundred years due to low sedimentation rates as well as drilling and anthropogenic disturbances (Lang and Wolff, 2011).

Terrestrial paleoenvironmental records registering the entire Holocene, are abundant in southeastern Iberia (Carrión et al., 2007, 2010;

García-Alix et al., 2012, 2017; 2021; Jiménez-Moreno and Anderson, 2012; Toney et al., 2020; Ramos-Román et al., 2018; Manzano et al., 2019; López-Avilés et al., 2022, among others). However, continuous Holocene records are scarce in the lowlands of southwestern Iberia (Fletcher et al., 2007; Manzano et al., 2018, 2019b; Schröder et al., 2020). Therefore, with this study we increase our knowledge about Holocene paleoenvironmental evolution in southwestern Iberia, providing new insights about the paleohydrological changes in the region during the last 12 ky through the sedimentary record of an environmentally-vulnerable playa-lake system.

2. Material and methods

A 158 cm-long sedimentary core (LB-15–01) was retrieved in 2015 with a Livingstone piston corer in the depocenter of the LB. Several drillholes with no sediment recovery show that the sedimentary infilling of the basin is ~2.5–3 m in thickness and the Miocene/Triassic basement is found at that depth in the central area of the LB depression. Among the six drives (sections) retrieved, four displayed some compaction during drilling and their real lengths were reconstructed to the real coring depths. The core was split, described and photographed at the Department of Stratigraphy and Paleontology of the University of Granada, where it is currently stored at 4 °C. Subsequently, magnetic susceptibility (MS) was measured at 0.5 cm intervals with a Bartington MS2E meter in SI units (x 10^{-4}) (Fig. 2).

The chronology of the LB-15–01 record was established by $^{239+240}$Pu activity profile in the topmost ~7.4 cm along with eight AMS radiocarbon dates obtained from 11.5 cm to 136.1 cm depth (Table 1). A pretreatment with HCl 1 N and HF 1 N was performed on the samples in order to concentrate their low organic content for radiocarbon analyses. Radiocarbon dates were calibrated into calendar years using the IntCal20.14c curve (Reimer et al., 2020) (Table 1). A Bayesian age-depth model including all these chronological data was calculated using the "Rbacon" R-based package (version 2.5 - October 2020 Blaauw and

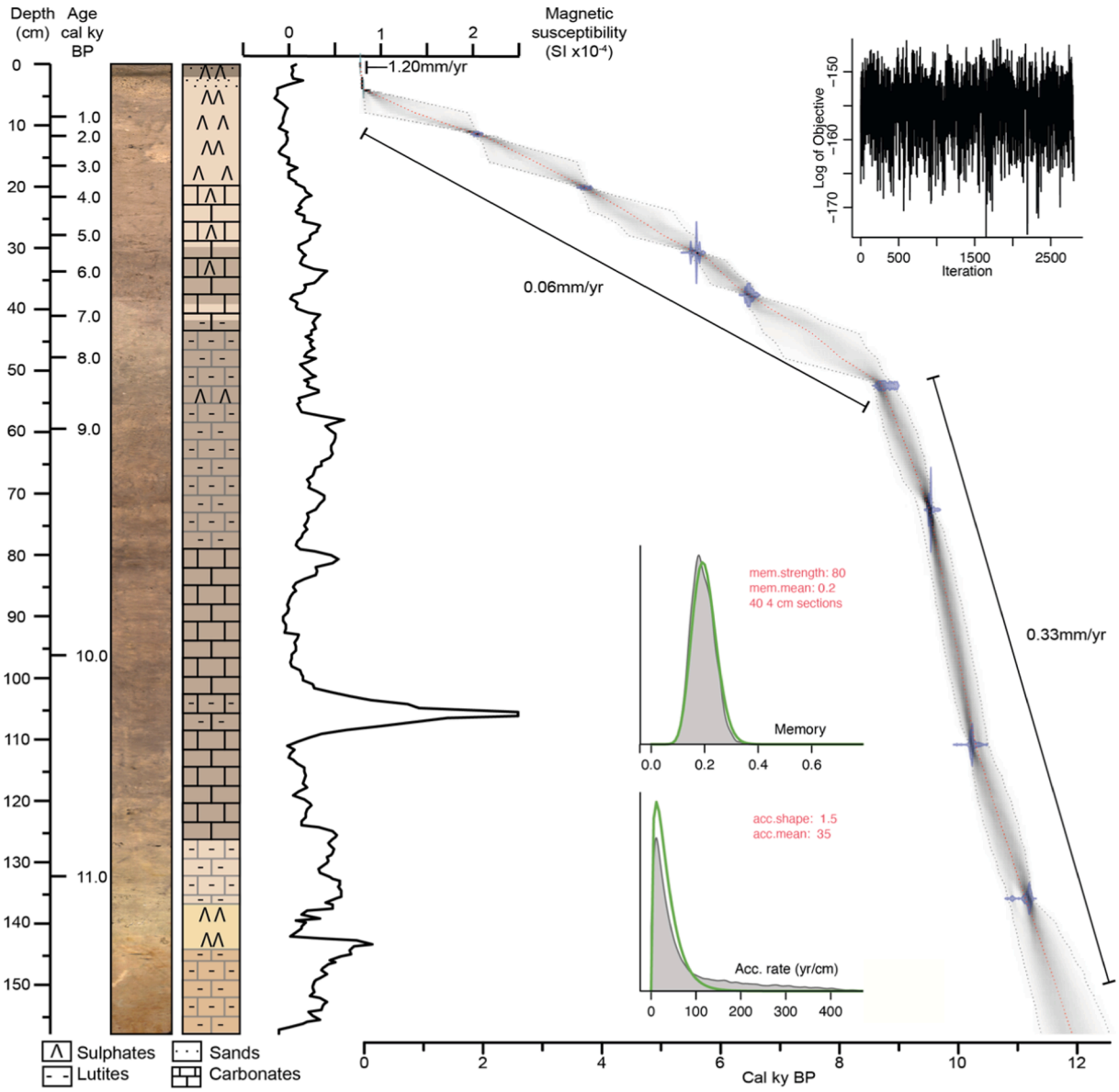

Fig. 2. Stratigraphic column, magnetic susceptibility profile (MS in SI units) and Bayesian age-depth model (95% confidence interval and red median line) of the LB-15–01 record. The calibrated ^{14}C dates and their uncertainties are represented in blue color. The accumulation rate plot shows the prior and posterior distribution of the accumulation rate (green and grey lines respectively). The memory plot represents the prior and posterior distribution of the model memory (green and grey lines respectively). The log-posterior time-series exhibit a stable model. The sediment accumulation rates (SARs) for the different sections of the core are also indicated. (For interpretation of the references to color in this figure legend, the reader is referred to the web version of this article.)

Table 1
Chronological data of the LB-15–01 core. $^{239+240}$Pu activity profile (LB-xxx samples) and radiocarbon ages (BETA-xxx samples) calibrated with Calib 8.2 (http://calib.org/calib/) and the IntCal20.14c curve (Reimer et al., 2020).

Sample ID	Depth (cm)	^{14}C Age (^{14}C yr BP)	$^{239+240}$ Pu (Bq/kg)	σ (Bq/kg)	Calibrated 2σ age (Cal yr BP)	Calibrated median age (Cal yr BP)
Surface	0					-65
LB-218	0.27		0.144	0.037		
LB-219	0.82		0.154	0.035		
LB-220	1.36		0.255	0.028		
LB-221	1.91		0.170	0.035		
LB-222	2.45		0.225	0.037		
LB-223	3.00		0.168	0.023		
LB-224	3.54		0.217	0.103		
LB-225	4.09		0.508	0.076		-13/-14
LB-226	4.63		0.301	0.040		
LB-227	5.18		0.214	0.039		
LB-228	5.72		< 0.1			
LB-229	6.27		< 0.1			
LB-230	6.81		< 0.1			
LB-231	7.36		< 0.1			
BETA −560864	11.45	1970 +/- 30			1994–1865	1920
BETA −487117	20.20	3450 +/- 30			3829–3637	3712
BETA −563349	30.80	4860 +/- 30			5653–5488	5602
BETA −560866	37.70	5700 +/- 30			6565–6406	6479
BETA −563350	52.50	7930 +/- 40			8981–8631	8769
BETA −487118	72.70	8560 +/- 30			9550–9495	9534
BETA −560868	111.00	9070 +/- 40			10276–10180	10229
BETA −487119	136.10	9740 +/- 40			11238–11104	11188

Christen, 2011) (Fig. 2). The Gelman and Rubin Reduction Factor (<1.05), the convergence test and the stable log-posterior time-series suggest a reliable model and good fitting (Fig. 2). The Early–Middle Holocene and the Middle–Late Holocene boundaries have been taken at 8.2 and 4.2 cal ky BP, according to the Holocene INTIMATE subdivision (Walker et al., 2012).

The organic elemental composition of bulk sediment was used to interpret the main features of the organic fraction in the LB-15–01 record. The low organic content in all the samples prevented additional studies, such as biomarkers or organic matter isotope analyses. A total of 152 samples taken at ~1 cm intervals were freeze-dried and decarbonated overnight by means of acid digestion (HCl 1 N). Afterwards, samples were rinsed and centrifuged with Milli-Q water until a neutral pH and freeze-dried again. The elemental composition (CN) of the samples was measured in the decarbonated fraction by means of a Themo Scientific Flash 2000 elemental analyzer at the Centre for Scientific Instrumentation of the University of Granada (CIC-UGR), Spain. The difference in weight between bulk and decarbonated samples provided the percentage of the carbonate fraction in the sample. The total content of C and N was recalculated to the weight of the original bulk sediment. Atomic C/N ratios were obtained from the total organic carbon (%TOC) and the total nitrogen (%TN) content.

High-resolution elemental profiles were obtained using X-Ray fluorescence (XRF) core scanner analyses throughout the sedimentary record with an Avaatech XRF core Scanner at the XRF-Core Scanner Laboratory of the University of Barcelona, Spain. The core was scanned at a resolution of 0.5 cm with two different settings: 1) 10 s count times at 10 kV X-ray voltage and 700 μA X-ray current for light elements (in our case Al, Si, S, K, Ca, Ti, and Fe), and 2) 35 s count time at 30 kV X-ray voltage and 1300 μA X-ray current for heavy elements (Zr, Sr in our case). Check points were analyzed in triplicate every 50 analyses. Results were expressed in counts per second – cps – (intensity) as well as normalized for the total sum of cps in order to minimize the effect of the water content, density and/or the sediment surface conditions (Bahr et al., 2014). Other elements were discarded due to low cps yield or their noisy signal.

Geochemical inorganic analyses were also performed on 14 discrete sediment samples to check the results of the XRF core scanner analyses. About 0.1 g of pre-powered and homogenized sample were dissolved with 2 ml of 69 % HNO_3 and heated at 130 °C until evaporation. Subsequently, 3 ml of HF were added and heated at 130 °C until evaporation. Then, 1 ml of 69 % HNO_3 was added and heated at 130 °C until evaporation too. This last step was repeated twice. Afterwards, 4 ml of 69 % HNO_3 and ~15 ml of Milli-Q water were added and heated at 80 °C for 1 h. Lastly, when the samples cooled down, each sample was diluted with Milli-Q water in 100 ml flasks and divided in two aliquots for both Inductively coupled plasma mass spectrometry (ICP-MS) and Inductively coupled plasma atomic emission spectroscopy (ICP-OES) analyses. Major elements (Al, K, Fe, Ca, Mn, Mg, Ti, S) were measured with an ICP-OES Perkin-Elmer Optima 8300 (Dual View) equipped with an autosampler Perkin-Elmer S10 at the CIC-UGR. Trace elements were measured with an ICP-MS Perkin-Elmer Sciex Elan 5000 spectrometer, using Re and Rh as internal standards at the CIC-UGR.

X-Ray diffraction (XRD) on sediment samples allowed the identification of different mineral phases. Thirty-seven samples throughout the core were analyzed with the Bruker D8 Discover diffractometer equipped with a Pilatus3r 100 K-A detector with Cu-Kα radiation and automatic slit at the CIC-UGR. Scans were run from 5° to 80° 2θ at 0.02° steps. Semi-quantitative estimations of mineral abundance were obtained using Xpowder (Martin, 2004) and Match! (Putz and Brandenburg, 2021) software packages.

3. Results

3.1. Chronology and sedimentary rates

The $^{239+240}$Pu activity profile obtained in the topmost ~7.4 cm of the LB-15–01 core reached a maximum (0.508 ± 0.076 Bq/kg) at ~4.09 cm depth. This maximum in $^{239+240}$Pu activity was related to a global fallout peak caused by nuclear weapon tests, suggesting an age around -13/-14 cal yr BP (1963/1964 yr CE) for this depth (Ketterer et al., 2004) (Table 1). Eight radiocarbon dates between 11.5 and 136.1 cm depth provided an age from ~1.9 to 11.2 cal ky BP for this interval (Table 1). There are no age-inversions.

The Bayesian age-depth model obtained from the $^{239+240}$Pu activity profile and the radiocarbon samples shows that the LB-15–01 sediment core records the last ~11.9 cal ky BP in 158 cm (Table 1 and Fig. 2). Two main changes are observed in the sediment accumulation rates (SARs):

at ~52 cm (~8.6 cal ky BP) and at ~3.8 cm (-30 – −35 cal yr BP, 1980–1985 yr CE). The mean accumulation rates for these periods are: 0.33 mm/yr from 158 to 52 cm (~11.9–8.6 cal ky BP), 0.06 mm/yr from 52 to 3.8 cm (~8.6 cal ky BP – 1980–1985 CE), and ~1.20 mm/yr for the last 3.8 cm (the last ~30–35 years) (Fig. 2).

3.2. Lithology, magnetic susceptibility (MS) and overall record description

The LB-15–01 core shows fluctuations in the content of evaporites and siliciclastic sediments throughout the sedimentary record. The grain size is lower at the bottom of the core, and lutite-size sediments predominate from the bottom of the core until ~42.5 cm depth (Fig. 2; ~7.3 cal ky BP). Brown lutites are found from the bottom of the core until ~144 cm depth (Fig. 2; ~11.4 cal ky BP), light grey lutites predominate from 137 to 126.4 cm (~11.2–10.8 cal ky BP) and dark grey lutites from 77 to 42.5 cm (Fig. 2; 9.6–7.3 cal ky BP). Carbonate is the most abundant mineral phase from the bottom of the core until the last ~20–17 cm (Fig. 2; ~3.6–3.1 cal ky BP). The darkest color is displayed at the top 2 cm where organic content slightly increased (brown color). The MS record shows the highest values in the first part of the record - from ~158 to 58 cm (Fig. 2) - covering the Early Holocene until ~8.9 cal ky BP, agreeing with the maximum siliciclastic content (see section 3.4), with a gradual decline towards the top of the record (Fig. 2) together with the siliciclastics (Fig. 3). This MS decreasing trend changes at the top of the record with a sharp increase at 3.8 cm depth (Fig. 2; ~1980–1985 CE). Gypsum crystals can be observed between 142 and 137 cm (11.4–11.2 cal ky BP), 56.6 to 55.5 cm (8.9–8.8 cal ky BP), 45.5 to 44.5 cm (7.7–7.6 cal ky BP), 35.9 to 35.5 cm (~6.2 cal ky BP), at 31 cm (~5.6 cal ky BP), and above 28 cm (~5.0 cal ky BP), especially in the uppermost 19 cm (the last ~3.5 ky) (Fig. 2).

3.3. Organic geochemistry

The organic content is generally low throughout the record, with TOC values lower than 1.4 % (Fig. S1). The lowest TOC values of the core occur from the bottom of the core until ~137 cm depth (before 11.2 cal ky BP), with TOC values ranging from 0.03 to 0.19 %. TOC values in the rest of the record range from 0.14 to 0.35%, but there are occasional increases at 24 cm depth (~4.4 cal ky BP: 1.4 %TOC) and in the last ~10 years of the record (0.60–0.73 %TOC) (Fig. S1).

C/N atomic ratios (hereafter C/N ratios) range from 4.1 to 16.9. Values lower than 10 occur from the bottom of the core to 129 cm depth (~10.9 cal ky BP), with some occasional exceptions, at ~8.3, 8.0, 4.4 cal

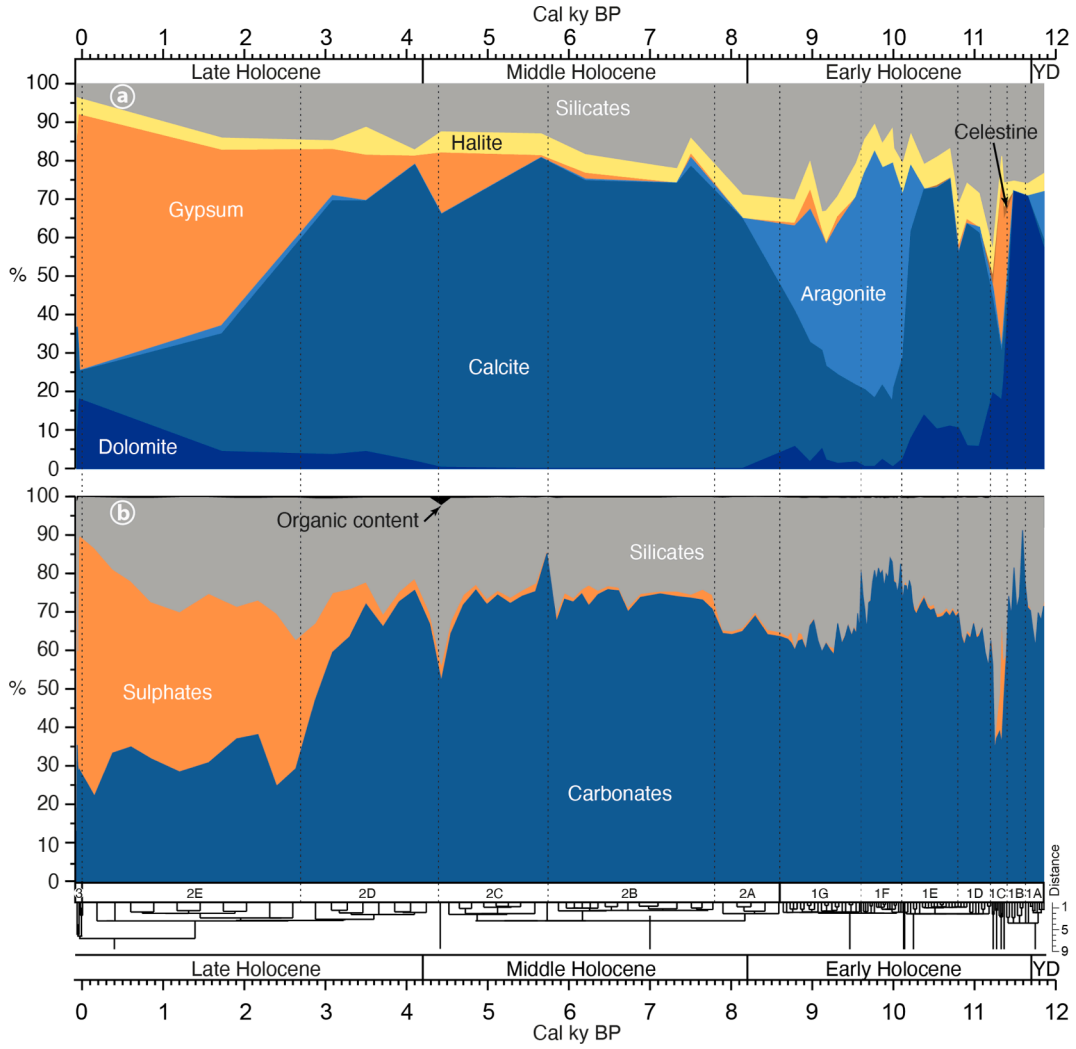

Fig. 3. Qualitative evolution of the main mineralogical phases and organic matter content in the LB-15–01 record along with the different unit/subunits obtained from a stratigraphically-constrained cluster analysis performed on the different proxies (MS, SAR, carbonate content, silicate content, sulphate content, %TOC, and C/N ratio). **a)** XRD analyses. **b)** Mineral phases reconstructed from the decarbonation analyses (carbonates), relative abundance of the main elements in the XRF core scanner analyses (Fe, Al, Si, K, Ti, and Zr for the siliciclastic content, and S for the sulphate content), and total organic matter reconstructed from the %TOC using the Van Bemmelen factor (Nelson and Sommers, 1983). Note the low sample resolution in the XRD analyses.

ky BP, and from ~3.9 cal ky BP to the present (Fig. 4g and S1). An increase in 4–5 units from the lowest values reached in the record (C/N = 4.1) is observed in the last 6 cm (last 400 years) (Fig. 4g and S1). The highest C/N values occurred in the Early Holocene (from ~10.9 to 8.4 cal ky BP), with values ranging from 10.1 to 15.9, and in the Middle Holocene (from ~7.9 to 4.7 cal ky BP), with values ranging from 11.5 to 16.9 (Fig. 4g and S1).

3.4. Inorganic geochemistry

3.4.1. Carbonate content

The carbonate content is higher than ~56 % from the bottom of the record until 17 cm depth (~3.1 cal ky BP) and only short intervals from ~11.4 to 11.2 cal ky BP and at ~4.4 cal ky BP (~144, 137, and 24 cm depth, respectively) showed a significant carbonate decrease (Figs. S1, 3b and 4f). During these periods of high carbonate content, values usually range from ~60 to 75 %. Values exceed 80 % at ~11.6 cal ky BP (when the highest carbonate content in the record is reached, 91.2%), at 11.5, 10.1, 10.0, from 9.9 to 9.8, at 9.6, and at ~5.7 cal ky BP (Figs. S1, 3b and 4f). The carbonate content declines after ~4.1 cal ky BP (22.5 cm depth) (Figs. S1, 3b and 4f). Carbonate contents lower than 40 % are registered in the latest Holocene (from 2.7 cal ky BP -14.5 cm depth- to the present), with the lowest values at ~2.4 (24.7 %) and 0.15 (22.1 %) cal ky BP (Figs. S1, 3b and 4f).

3.4.2. Major and trace elements

The comparison between the inorganic geochemical data (Al, Ca, K, Ti, Fe, S, Zr and Sr) obtained from ICP analyses in discrete samples and those from the XRF core scanner exhibit a high and statistically significant positive correlation ($r > 0.77$, $p < 0.002$), supporting the use of the XRF core scanner data to reconstruct high resolution trends in the studied record (Table S1). ICP data of Al, Ca, K, Ti, Fe, S, Zr and Sr are summarized in Table S2.

A correlation matrix and a principal component analysis (PCA) were performed to assess the relationship between nine elements (Al, Si, K, Ti, Fe, Zr, Sr, Ca, and S) analyzed by means of the XRF core-scanner. Both analyses show a significant correlation/grouping of Al, Si, K, Ti, Fe, and Zr (siliciclastic group) (Table S1 and Fig. S2). The relationships between Ca and S (evaporitic group) are more complex, showing an overall negative correlation with the siliciclastic group. Sr failed to display any correlation with the other elements (Table S1 and Fig. S2). Similarly, the correlation of the different elements analyzed in discrete samples show that the Al, K, Ti, Fe, and Zr, usually related to siliciclastic deposits, display a significant positive correlation ($r > 0.95$, $p < 0.0001$), and that Ca and S exhibit negative correlations with these siliciclastic elements, but less significant ($r < -0.60$, $p < 0.02$) (Table S1). The Sr correlations with other elements are moderate and do not show statistically significance (Table S1). The PCA analyses on XRF core scanner data show that the first three PCs explained 93.8 % of the total variance. PC1 explains 69 % of the variance, and two main groups of elements are observed: the siliciclastic group that exhibited high positive correlation loadings, contrasting with the high negative correlation loadings of S and Ca (Fig. S2). The PC2 explains 13.6 % of the variance and shows high, but inverse correlation loadings for Ca and S (Fig. S2). The PC3 explains 11.2 % of the variance and only shows high positive loading for Sr (Fig. S2).

The signal of Ni, Cu, Zn, and Pb obtained from XRF core scanner analyses is very low, pointing towards a scarce content of these metals in the LB-15–01 record. The content of these elements obtained from ICP-MS analyses displays a similar distribution as the elements of the siliciclastic group throughout the record, exhibiting a gradual decreasing trend since the Early Holocene (Table S3).

The Al, Si, K, Ti, Fe, and Zr content is high from the bottom of the core to ~10.7 cal ky BP -123.5 cm depth- (except for a short event between ~11.4 and 11.2 cal ky BP) and from 9.6 to 7.8 cal ky BP (~77–46 cm). After ~7.3 cal ky BP (~42.5 cm depth) there is a significant decreasing trend and only a sharp increase in these elements is observed in the last ~35–30 years of the record (Fig. S3).

S content is low during the Early and Middle Holocene, and there is only a sharp rise at ~11.4 and 11.2 cal ky BP (144–137 cm). S content starts increasing at ~4.4–4.3 cal ky BP (24 cm depth), especially after 4.1 cal ky BP (22.5 cm depth) until -41 cal yr BP. Afterwards, it decreases slightly until present (Fig. S3).

The lowest Ca values occur from the bottom of the record until ~10.8–10.7 cal ky BP (~126.0–123.5 cm depth). After this point, low Ca content is observed from 9.6 to 8.0 cal ky BP (~77–47 cm), and after ~3.5 cal ky BP (19 cm depth) when the Ca content decreases gradually (Fig. S3). The Ca content fails to show a clear relationship with the carbonate content since it represents, at least, the combination of both carbonates and gypsum.

Sr depicts constant values throughout the record. There are only three intervals when Sr increases: between 11.6 and 11.0 (~149–132 cm), between 10.2 and 8.9 (~108–57 cm), and between 7.8 and 6.6 cal ky BP (~46–38.5 cm; Fig. S3).

3.4.3. Mineralogy

Eight mineralogical phases have been identified in the LB-15–01 record: silicates (quartz and clays), carbonates (calcite/magnesian calcite, dolomite and aragonite), and other evaporites (gypsum, halite and celestine) (Fig. 3a and S4). The highest concentration of silicates occurs in the Early Holocene, in the interval between ~10.7 and 9.6 cal ky BP (~124–77 cm). Silicates exhibit a decreasing trend after ~8.0 cal ky BP (~47.5 cm depth) (Fig. 3a and S4). The halite content is very homogeneous throughout the record, with a mean value of 6.5 ± 2.4 %, reaching maximum values in the last decade (Fig. 3a and S4). Celestine only occurs at two short intervals, from 11.4 to 11.2 (144–137 cm) and at ~10.7 cal ky BP (~124 cm depth) (Fig. 3a and S4). Gypsum is found in different periods throughout the record and shows significant concentrations between 11.4 and 11.2 cal ky BP (144–137 cm), at ~9.0 cal ky BP (~60 cm depth), and after ~4.4 (~24 depth cm), especially after 4.1 cal ky BP (~22.5 cm depth), reaching the highest concentrations in the record after ~1.7 cal ky BP (~11 cm depth) (Fig. 3a and S4).

The carbonate content is high from the bottom of the record until ~3.1 cal ky BP (~17 cm depth) (Fig. 3a and S4). There is only a significant drop during a shortly episode between ~11.4 and 11.2 cal ky BP (144–137 cm), when sulphates are most abundant (Fig. 3a and S4). Different carbonate phases occur throughout the record. Dolomite predominates from the bottom of the record until 11.3 cal ky BP (~141 cm depth) with concentrations higher than 57 % (Fig. 3a and S4). An increase in the calcite content occurs later on until ~10.1 cal ky BP (~101.5 cm), when the aragonite content sharply increases, being the major carbonate phase until ~8.8 cal ky BP (~55 cm). Aragonite registers the highest concentration between 10.1 and 9.6 cal ky BP (Fig. 3a and S4). After 8.6 cal ky BP, the presence of aragonite is almost negligible. Subsequently, calcite becomes the most important carbonate phase again. Carbonates decrease along with the calcite content after ~4.1 cal ky BP (~22.5 cm), while the dolomite phase gradually increases until recent times (Fig. 3a and S4).

The Pearson correlation between silicate, sulphate and carbonate contents deduced from XRD data and the same phases deduced from XRF core scanner and decarbonation analyses is high ($r = 0.83$ silicates, $r = 0.97$ sulphates, and $r = 0.92$ carbonates, $p < 0.0001$).

4. Discussion

4.1. Data integration in the LB-15–01 record

Constructing age-depth models based on radiocarbon dating in lakes with low organic inputs/production are challenging (Fowler et al., 1986; Valero-Garcés et al., 2000b), and methodological procedures to concentrate the organic matter usually need to be applied. Apart from the scarce organic content, another potential issue for radiocarbon chronologies obtained from aquatic materials in lacustrine systems,

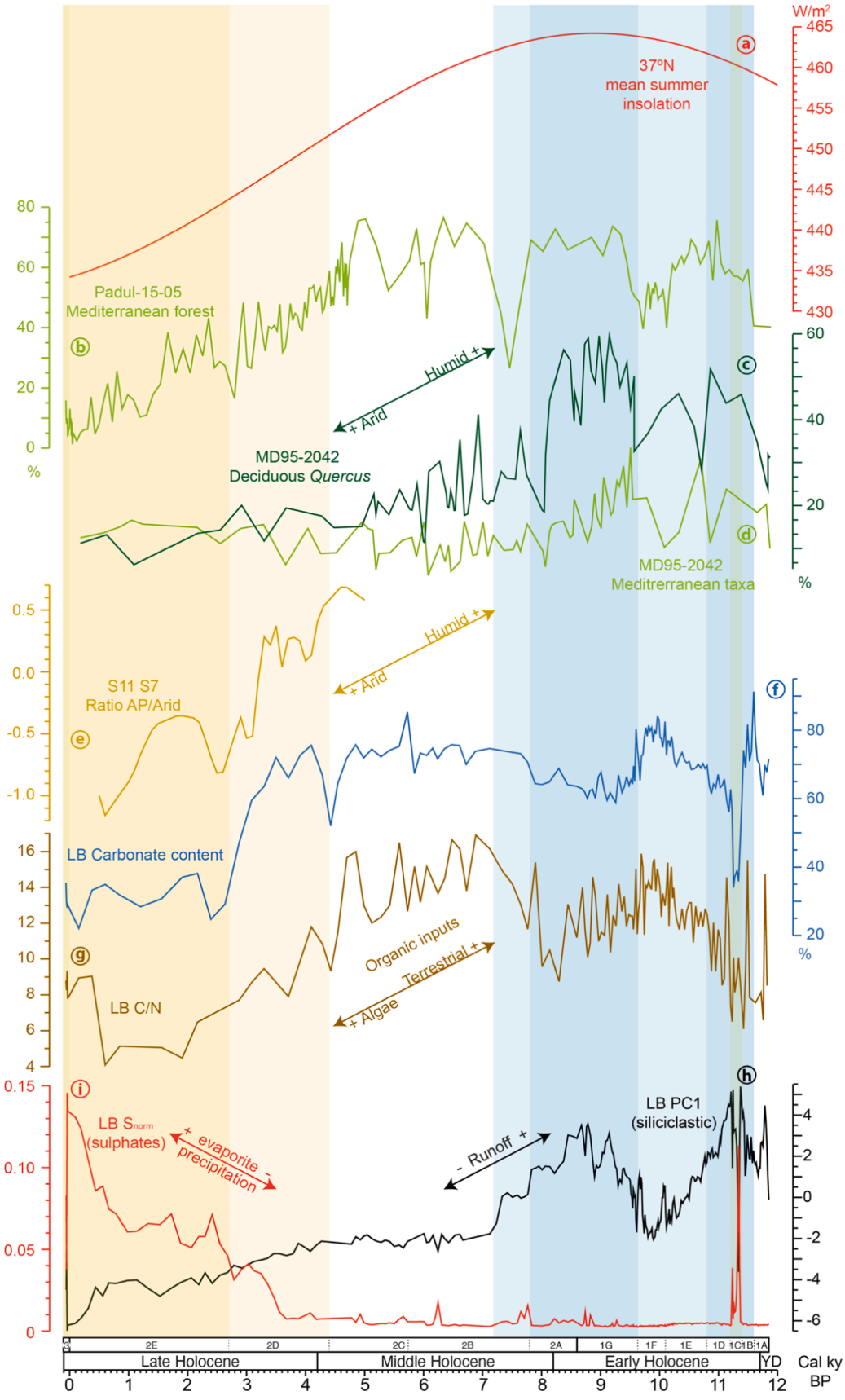

Fig. 4. Comparison of several paleoenvironmental proxies from southern Iberian Peninsula with the mean summer insolation at 37°N. **a)** Mean summer insolation at 37°N (Laskar et al., 2004). **b)** Mediterranean taxa deduced from palynological analyses of the Padul-15–05 record, southeastern Iberia (Ramos Román et al., 2018 a,b). **c)** Deciduous *Quercus* and **d)** Mediterranean taxa evolution deduced from palynological analyses of the MD95-2042 record, southwestern Iberia (Chabaud et al., 2014). **e)** Synthetic AP/arid curve (AP-arid)/(AP + arid) representing the relationship between arboreal and arid pollen taxa from sediment cores S11 and S7 taken from a marshland area in the Guadalquivir valley, southwestern Iberia (Jiménez Moreno et al., 2015). **f)** Record of the carbonate content, **g)** the C/N atomic ratio, **h)** the PC1 (interpreted as siliciclastic content), and **i)** S_{norm} (interpreted as sulphate content) in the LB-15–01 core. The different unit/subunits were obtained from a stratigraphically-constrained cluster analysis in the LB-15–01 record (see Fig. 3).

especially in saline lakes, can be the fresh water reservoir effect (Olsson, 1979), also known as hard-water effect (Deevey et al., 1954), due to the contribution of older inorganic dissolved carbon. The potential adsorption of old inorganic carbon by aquatic organisms (via photosynthesis or carbonate shell precipitation) could provide older radiocarbon ages (Olsson, 1979; Deevey et al., 1954). However, previous works have shown that areas fed by shallower and younger groundwaters are less affected by these alterations (Höbig et al., 2016). Groundwater discharge from the O-LL aquifer to the LB playa-lake is expected to have a relatively high renovation rate, since the hydrogeological watershed (i.e., the recharge area) of the O-LL aquifer is adjacent to the wetland, in addition to the low residence times of the O-LL aquifer (Beltrán et al., 2012). Another potential issue for radiocarbon chronologies from bulk organic sediment in lacustrine systems with a mixture of terrestrial aquatic materials, is the potential reworking of older terrestrial organic materials from the catchment soils (Schoute et al., 1981). The combination of both effects in radiocarbon chronologies based on terrestrial and aquatic materials would cause age inversions (Valero-Garcés et al., 2000b). Nevertheless, the age-depth model obtained in the LB-15–01 record is very coherent and no age inversions have been detected in the radiocarbon dates. The topmost section of the record is characterized by bulk organic contribution coming from aquatic algae (radiocarbon samples at 11.45 and 20.2 cm depth with C/N ratios 4.5 and 7.9, respectively) and a mixture of aquatic and terrestrial material (radiocarbon samples at 30.8 and 37.3 cm with C/N ratios 16.5 and 16.7, respectively). This section shows a constant SAR of 0.06 mm/yr (Fig. 2). Similarly, in the bottom part of the record, the C/N ratios of the radiocarbon samples suggest a mixture of aquatic and terrestrial material (C/N ratios ranging from 12.1 to 15.2). This section also shows a homogenous SAR (0.33 mm/yr) (Fig. 2).

A cluster analysis performed on the most important proxies analyzed in LB-15–01 record allowed the identification of three main units and subunits (Fig. 3 and Table S4). A high SAR stage (unit 1) from ~11.9 to 8.6 cal ky BP (~3.3 ky) registered more than 1 m of sediment accumulation (Fig. 2) with a significant contribution of siliciclastic and carbonate materials (Figs. 3, 4f, 4 h and Table S4). The first part of this unit, from ~11.9 to 11.4 cal ky BP, displayed high carbonate and siliciclastic content (subunits 1A and 1B; Figs. 3, 4f, 4 h and Table S4). The siliciclastic contribution, deduced from the mineralogical and geochemical signatures, registered two declines in unit 1. The oldest one was in subunit 1C. This subunit (~11.4–11.2 cal ky BP) showed a short and abrupt siliciclastic drop from ~11.4 to 11.3 cal ky BP, followed by a sharp increase. These fluctuations were coeval with abrupt oscillations in the sulphate content and with a significant carbonate reduction (Figs. 3, 4f, 4 h, 4i and Table S4). The siliciclastic and carbonate content remained high between 11.2 and 10.8 cal ky BP (subunit 1D) (Figs. 3, 4f, 4 h and Table S4); however, another slighter but longer decrease in siliciclastics was detected between ~10.8 and 9.6 cal ky BP (subunits 1E and 1F) (Figs. 3, 4f, 4 h, 4i and Table S4).

A low SAR stage (unit 2) occurred from ~8.6 ky to recent times with a sediment accumulation of ~50 cm (Fig. 2 and Table S4). This unit began with a gradual decrease in siliciclastics (subunit 2A), although this was moderately high until ~7.3 cal ky BP (subunit 2B; Figs. 3, 4h and Table S4). Sulphates were minor components in the record until ~4.4–4.3 cal ky BP, and their content especially rose after ~4.1 cal ky BP, when the carbonate content started to decrease and a gradual increase in the dolomite phase occurred (subunits 2D and 2E; Figs. 3, 4g, 4i, 4 h and Table S4). Finally, a stage characterized by the highest SAR in the record (unit 3) can be identified in the last ~35–30 years with a deposit of ~3.8 cm of sediments (Fig. 2), agreeing with an abrupt siliciclastic increase (unit 3; Figs. 3, 4h and Table S4). The mineral phases identified show an overall inverse relationship between carbonates and sulphates throughout the record ($r = -0.81$, $p < 0.0001$).

4.2. Paleoenvironmental evolution of the Laguna de la Ballestera wetland

The age model for the LB-15–01 core shows an age of ~11.9 cal ky BP for the oldest sediments in this record, beginning at the Younger Dryas (YD)-Early Holocene transition. However, the origin of the LB depression and lake environment is older, according to the difference in depth between the bottom of the studied core (~1.5 m) and the Miocene/Triassic basement (~2.5–3.0 m). The extrapolation of the Early Holocene SAR of LB-15–01 core suggests that sedimentation in the lacustrine system could have started during the Bølling–Allerød and that aeolian deflation could have acted as an important agent on the depression formation (Moral Martos, 2016) during previous stages of extreme arid conditions in southern Iberia, such as the Heinrich Stadial 1 and/or the Last Glacial Maximum (Rodrigo-Gámiz et al., 2011; Camuera et al., 2019, 2021; García-Alix et al., 2021).

The oscillations in SARs, siliciclastic, carbonate and sulphate contents observed in the Holocene record of LB can be related to changes in the hydrological regime of the water body, specifically changes in the water balance (runoff *vs* groundwater or discharge *vs* recharge), and/or a shift from an open lacustrine area to a closed (endorheic) system. Present groundwater in LB is brackish and rich in chloride, sulphate and bicarbonate from the dissolution of Triassic halite and gypsum as well as from Miocene marls and calcarenites (Rodríguez-Rodríguez et al., 2008). Therefore, the high evaporite content in the LB-15–01 record, such as carbonates until ~4.1 cal ky BP and gypsum after 4.4 cal ky BP and, specially, from 4.1 cal ky BP (Figs. 3, 4f and 4i), means that groundwater contribution was significant throughout the record and gained importance when runoff (indicated by siliciclastic content) gradually decreased.

In this way, highest humidity can be interpreted for the Early Holocene (until ~8.6 cal ky BP), which generated high catchment runoff (high SAR and siliciclastic input) and also significant groundwater input as a consequence of the high piezometry (high carbonate precipitation from groundwater enriched in bicarbonates) (unit 1; Figs. 2, 3, 4f, 4 h, 5a-b and 6). LB would have then registered the highest lake levels and formed part of a wider palustrine environment covering the entire La Lantejuela basin, with a likely extension of more than 300 km^2 (Fig. 5a-b and 6). Present day streams draining water into the LB area come mainly from the southern reliefs, converging in the center of La Lantejuela depression and flowing out westwards. The most important of such streams are the Peinado and Salado streams (Fig. 6). The Peinado-Salado drainage system could have also worked during the Early Holocene, probably with less outflow, feeding the depression where the main playa-lakes are situated. At that stage, the Salado and Peinado streams periodically flooded, inundating the depression and forming a continental fan delta at an approximate altitude of 153 m a.s.l. (Fig. 6a). The present-day hydrology has been drastically modified by the channeling of the Salado stream (Fig. 6b). The location of the LB wetland in the central part of this depression can explain the presence of fine siliciclastic sediments (lutites) during the Early Holocene instead of coarser siliciclastic materials (unit 1; Figs. 2, 3 and 4h). Detritic carbonate inputs could also have occurred in this phase of high humidity. However, carbonates and siliciclastic elements show anticorrelation (e.g., PC1 *vs* carbonate content $r = -0.58$, $p < 0.0001$) during this high-to-moderate humid period until ~6.2 cal ky BP, discarding important detritic contribution of carbonates during this period of significant runoff. This anticorrelation was probably related to the alternation of periods when high runoff, indicating more siliciclastic input to the LB, diluted the contribution of groundwater input (moderate carbonate precipitation), and the other way around (Figs. 3, 4f and 4 h). Although the carbonate content was generally high during this phase, changes in the carbonate mineralogical phases were also controlled by environmental variables; however, the mechanisms affecting the carbonate precipitation in lacustrine environments are still under debate (e.g., Roeser et al., 2016). In this way, the presence of dolomite from the bottom of the core until ~8.0 cal ky BP, but especially until 11.3 cal ky BP (subunits 1A-1C;

Fig. 3) could be related to important contributions of saline waters either via runoff or groundwater. Additionally, recent studies associated the aragonite precipitation in saline lakes to the presence of freshwater inputs and/or via oxidation of organic matter by sulfate-reducing bacteria and/or additional carbonate inputs (Ben Dor et al., 2021). Aragonite deposition in LB between ~10.1 and 8.8–8.6 cal ky BP (subunits 1F and 1G) could be associated with humid periods and high lake levels, as it has described in freshwater environments with brines mixes (e.g., Belmaker et al., 2019). In addition to this predominance of aragonite precipitation over calcite, fine siliciclastic materials were registered in LB during this period (Fig. 3). A similar association was explained in the Fuente de Piedra playa-lake (southern Iberia) by flocculation processes in a standing water body with fresh surface water inputs and saline/brackish groundwaters (Höbig et al., 2016).

An occasional and short period of enhanced aridity has been identified during the Early Holocene between 11.4 and 11.2 cal ky BP, especially from 11.4 to 11.3 cal ky BP (subunit 1C). This is based on the abrupt sulphate rise, reaching similar values as the ones registered in the Late Holocene, together with the significant decrease in the carbonate and siliciclastic contents, although siliciclastic rapidly increased from 11.3 to 11.2 cal ky BP (Figs. 3, 4f, 4 h and 4i). This episode of enhanced sulphate precipitation could have been produced by a short desiccation event in LB area.

The humid scenario in the Early Holocene was followed by drier climate conditions, indicated by runoff reduction deduced by the siliciclastic decrease that was gradual from ~8.6 to 7.8 cal yr BP (subunit 2A) and more abrupt after ~7.3 cal ky BP (subunit 2B onwards; Figs. 3 and 4h). Nevertheless, moderately wet conditions continued and thus important contribution of groundwater discharge with substantial amount of bicarbonate most likely occurred, deduced from the high carbonate content and the scarcity of gypsum until ~4.4–4.1 cal ky BP (subunits 2B and 2C; Figs. 3 and 4f). The abundance of carbonate compared to the low content of sulphates before ~4.1 cal ky BP suggests that low water levels, and thus annual desiccation was not common in LB before that age (Fig. 5c). However, occasional water level drops during the Middle-Late Holocene transition cannot be ruled out, coeval with occasional sulphate content rises (Figs. 3 and 4i). Also, this change possibly points out the independence of LB, as an endorheic playa-lake, from the La Lantejuela palustrine environment complex. This is a shift from a larger, and possibly semi-permanent lake system with sedimentological features similar to an inner-deltaic system to a smaller and seasonal LB playa-lake system with an independent watershed from the other playa-lakes of the La Lantejuela complex (Fig. 5c). Gypsum concentration gradually increased after 4.1 cal ky BP to the present (subunit 2D onwards; Figs. 3, 4i, 5d and 5e), suggesting more arid climate conditions coeval with a runoff decrease and more evaporation that

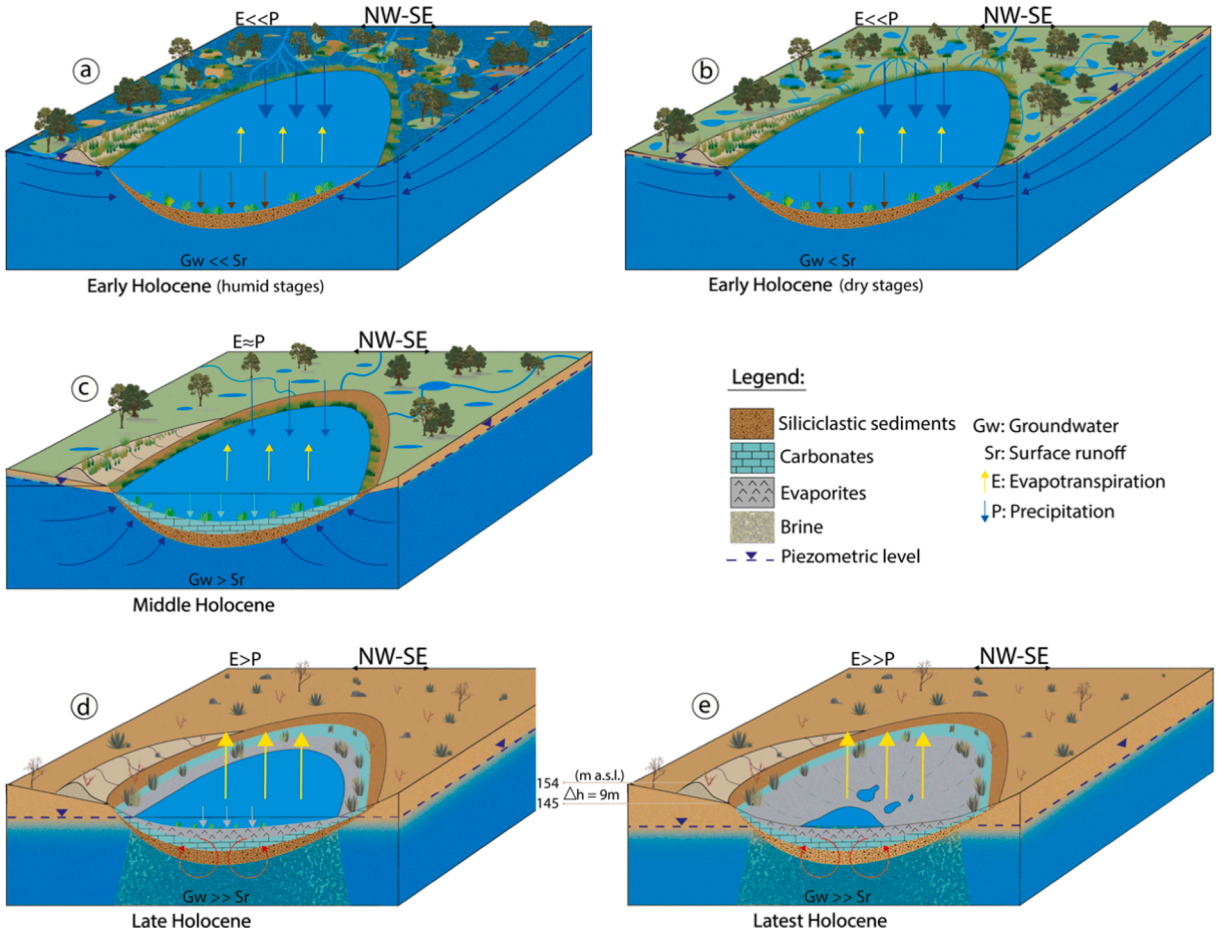

Fig. 5. Schematic evolution of LB wetland during the Holocene. **a-b)** Early Holocene: The main water input was surface water. The entire La Lantejuela basin was flooded during the humid stages **(a)** and the piezometric levels decreased during occasional drier stages **(b)**. **c)** Middle Holocene: Surface water and groundwater inputs are balanced (intermediate salinity and piezometric levels). **d)** Late Holocene (playa-lake): The main water input was groundwater discharge. Density-driven groundwater brine, caused by the high evapotranspiration, prevented from direct groundwater recharge in LB. **e)** Latest Holocene (playa-lake): The same scenario as **(d)** but with enhanced summer desiccation in the terminal stages of the playa-lake. See the text for further explanations. Gw: groundwater, Sr: surface runoff, E: evapotranspiration, P: precipitation. Yellow arrows represent evaporation, blue arrows represent different water inputs. Discontinuous lines represent intermittent flow and water arrows point the direction of the flow. (For interpretation of the references to color in this figure legend, the reader is referred to the web version of this article.)

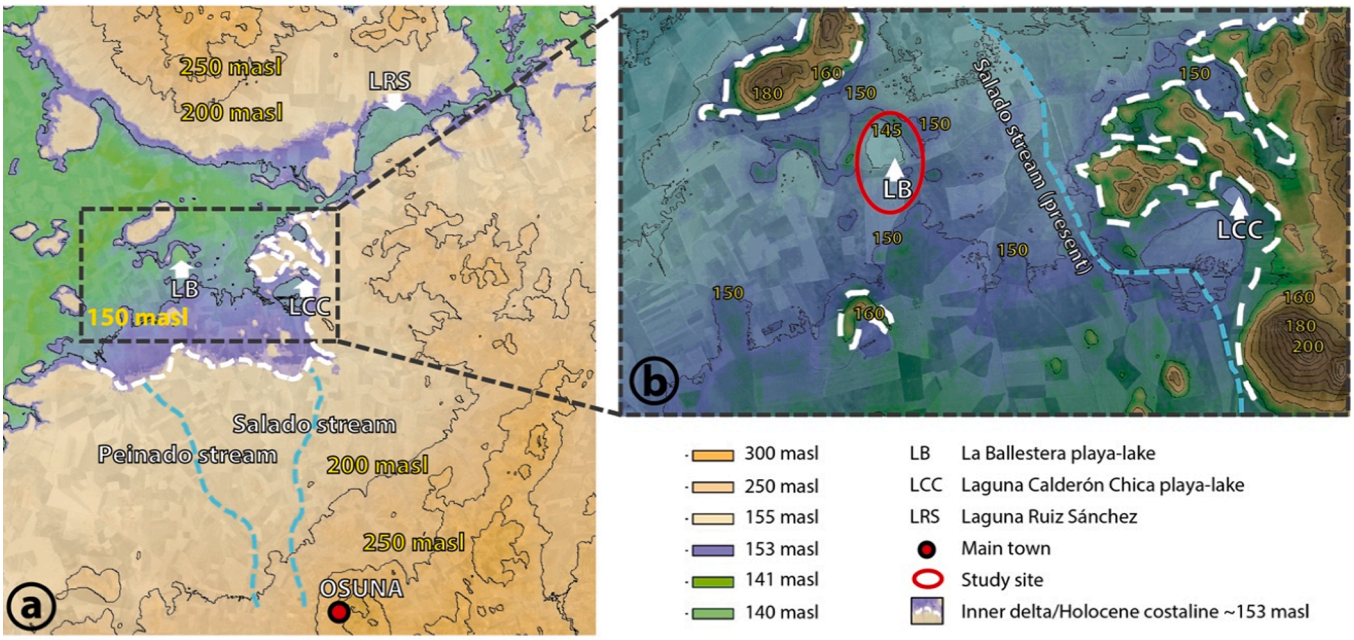

Fig. 6. Potential flooded area (purple and green colors) surrounding LB in La Lantejuela playa-lake system during the humid periods of the Early Holocene based on the presence of lacustrine sediments and the topography. The white dashed line delimits the boundary between the inner delta and the coastline. **a)** It includes the courses of the Salado and Peinado paleostreams. **b)** It includes the present (channelized) course of the Salado Stream. (For interpretation of the references to color in this figure legend, the reader is referred to the web version of this article.)

increased the salt concentration in groundwater and thus, brine development under each of the La Lantejuela playa-lakes (Fig. 5d and 5e). Sulphates were mostly abundant during periods when water salinity increased in the basin, probably related to more aridity and evaporation (Rodríguez-Rodríguez et al., 2008), being especially significant after 1.0–0.9 cal ky BP (beginning of the Medieval Climate Anomaly-MCA). Under this scenario of increasing sulphate precipitation, and especially after 0.4 cal ky BP, when the siliciclastic content dropped and the carbonate content was low (~30%) with notable dolomite presence (Figs. 3, 4f, 4 h and 4i), local summer desiccation in the playa-lake system was likely (Fig. 5e). Chlorides are also present throughout the record, only showing an increase in the last decade (Fig. 3). Since chlorides are highly soluble, they can be dissolved and precipitated at any depth in the studied deposits and thus cannot be used to reconstruct past environmental scenarios in this record.

Aeolian deflation could have acted during the desiccation stages described in the Late Holocene (Moral Martos, 2016). However, the constant SAR in the different parts of the record, including the Middle and Late Holocene (the last ~8.6 ky: units 2 and 1), the continuous $^{239+240}$Pu activity and radiocarbon profiles without age inversions, and the absence of erosive features in the LB-15–01 core suggest that the potential effect of aeolian deflation during these dry periods was probably negligible. Evaporitic crust and algal mats formed when the lake desiccated could have protected the lake floor from wind erosion.

Overall, low organic content (0.23 ± 0.12 %TOC) was registered throughout the core. Only at ~4.4 cal ky BP (1.4 %TOC) and in the last 15 years (0.6–0.7 %TOC) (Figs. 3 and S1) the organic content slightly increased. This means that primary productivity, from both aquatic and terrestrial sources, was not high in this playa-lake environment throughout the Holocene. The organic contribution to the sediments could have been masked by the high sedimentation rates (Meyers, 2003) during the first part of the record and during the last ~35–30 years (units 3 and 1; Fig. 2), but, in any case, figures would be lower than 0.01 mm/year of organic sedimentation (after correcting the TOC by the SARs).

C/N values, generally below ~9–10, showed that the source of organic matter in the core was mainly algae from the bottom of the record until ~10.9 cal yr BP (subunits 1A-1D; Fig. 4g). According to Meyers (2003), the source of organic matter would have primarily been a mixture between terrestrial and aquatic contribution after ~10.9 and until 3.9 cal ky BP, indicated by C/N ratios ranging from ~10 to 17 (subunits 1E-2D; Fig. 4g). C/N ratios started decreasing after 4.8 cal yr BP, coeval with a first drop in the carbonate content, and aquatic organic sources predominated after ~3.9 cal ky BP, agreeing with the timing of the carbonate content decrease until present (Fig. 4f). A sharp C/N increase (from 4.1 to 9) at 0.4 cal ky BP (subunit 2E; Fig. 4g) changed this decreasing trend, likely caused by some occasional inputs of terrestrial organic matter from the catchment. In any case, minor contribution of terrestrial organic matter has been observed throughout the record. This agrees with the environmental evolution deduced by the inorganic geochemistry results. The C/N ratios exhibit a general correlation with the carbonate content throughout the core ($r = 0.66, p < 0.0001$). This is probably related to the effect of the amount of bicarbonate on the algae development, especially in the Early and Middle Holocene. The siliciclastic content does not show any apparent correlation with the C/N ratios when analyzing the entire record. Nevertheless, a statistically significant anticorrelation ($r < -0.60, p < 0.0001$) is observed when this is assessed in the Early and Middle Holocene part of the record (from ~11.9 to 6.2 cal ky BP). This anticorrelation can be related to the nutrient availability in the aquatic environment triggered by runoff inputs. Runoff would have provided more nutrient supplies for the development of aquatic primary productivity (i.e., algae), and the other way around. A decrease in humidity during the Middle Holocene would have reduced the nutrient supply to the lake. In this scenario, the general correlation ($r = 0.68, p < 0.0001$) between C/N and the siliciclastic inputs during the last ~6.2 ky can be read as parallel fluctuations in both runoff and terrestrial organic matter inputs.

The long-term behavior of playa-lake systems, as well as of other groundwater dependent ecosystems, can be very different, even in the same region, depending on the hydrological functioning and characteristics of the aquifer. For example, the evaporitic record of Lagunas Reales playa-lake in central Spain, which is connected to a multilayer aquifer and only flooded in very rainy years, was not related to enhanced evaporation, but rather to higher groundwater levels during wet periods

(Mediavilla et al., 2020). Conversely, in the studied record of LB we have observed that sulphates mainly precipitated during the lowest water levels, which corresponded to stages of low runoff (less surface water availability), when the main water input comes from groundwater with high salt concentration. The sedimentary records of other evaporitic lakes in Andalusia such as Laguna de Fuente de Piedra (Málaga) and Zóñar Lake (Córdoba) (Martín-Puertas et al., 2009b; Höbig et al., 2016), follow a similar pattern as LB: more contribution of carbonates and/or siliciclastic inputs when water levels were high (high rainfall / groundwater discharge and/or reduced evaporation), and sulphate precipitation when the water supply was low and/or the evaporation was intense.

4.3. The paleoenvironmental record of LB in the context of the western Mediterranean

The general sedimentary evolution observed in the LB record since the YD-Early Holocene agrees with the general paleoclimatic trends described in the western Mediterranean and especially in the southern Iberian Peninsula, but it also provides unique information about the effect of climate variations on saline lakes. The LB catchment basin was characterized by high runoff (high siliciclastic and high SARs) during the Early Holocene, which agrees with the overall humid conditions observed regionally (unit 1; Figs. 2, 3 and 4h). Afterwards, the gradual runoff reduction in the LB catchment throughout the Middle Holocene, especially after 7.3–7.0 cal ky BP, and the subsequent enhanced gypsum precipitation in the Late Holocene (unit 2; Figs. 2, 3, 4h and 4i) agrees with many other studies from both southeastern and southwestern sectors of the Iberian Peninsula (Fletcher et al., 2007; Rodrigo-Gámiz et al., 2011; García-Alix et al., 2012, 2017; Chabaud et al., 2014; Jiménez-Espejo et al., 2014; Jiménez-Moreno et al., 2015; Ramos-Román et al., 2018a, 2018b; among others) and from the wider circum-Mediterranean region (Jalut et al., 2009) exhibiting an aridification trend during this period (Fig. 4b-e). Therefore, the LB record shows a regional response of the terrestrial wetland environments to the balance between precipitation/evapotranspiration during the Holocene that in southern Iberia was ultimately controlled by changes in summer insolation (Camuera et al., 2018, 2019; García-Alix et al., 2021) (Fig. 4).

4.3.1. Early Holocene

Subsequently to the latest Pleistocene, humidity started to increase in the western Mediterranean in the Early Holocene (Fletcher and Sánchez Goñi, 2008; Rodrigo-Gámiz et al., 2011; Zielhofer et al., 2017; Camuera et al., 2018, 2019, 2021; García-Alix et al., 2021; López Avilés et al., 2022, amog others), evidenced in the LB record by a short and occasional period of important runoff at the YD-Early Holocene transition (subunit 1A; ~11.8 cal ky BP; Figs. 3 and 4h) and two main episodes of significant runoff/erosion in the catchment basin: one from ~11.6 to 10.8 cal ky BP (subunits 1B and 1D) and another one from ~9.7–9.6 to 8.0–7.8 cal ky BP (subunits 1G and 2A) (Figs. 3 and 4h).

The first episode of significant runoff in the LB catchment, from 11.6 to 10.8 cal ky BP, was probably due to the response of the basin to enhanced humid conditions that actively eroded the surrounding landscape after the dry YD in the western Mediterranean (Fletcher and Sánchez Goñi, 2008; Rodrigo-Gámiz et al., 2011; Zielhofer et al., 2017; Camuera et al., 2018, 2019, 2021; García-Alix et al., 2021; López Avilés et al., 2022, amog others). This period also registered a regional vegetation response in southern Iberia to warmer and more humid conditions (Chabaud et al., 2014; Ramos-Román et al., 2018b). The abundance of carbonates during the humid Early Holocene and the low content of sulphates can also be interpreted as high contribution from groundwater and no lake desiccation (Figs. 3, 4h and 4i). This scenario could have changed briefly during a short episode between 11.4 and 11.2 cal ky BP (subunit 1C), when the carbonate content decreased and the sulphates increased abruptly along with a large fluctuation (drop/rise) in siliciclastics (Figs. 3 and 4f, 4 h and 4i). This short and abrupt arid episode, especially at the moment when the highest sulphate precipitation occurred (~11.4–11.3 cal ky BP) agrees with the timing of the Bond event 8 (Bond et al., 2001). This climatic event seems to have reduced rainfall in the western Mediterranean (Ramos-Román et al., 2018b), probably also causing fast and sharp high evaporative conditions in the LB basin. After this point there is no apparent synchronicity between the Bond events and occasional dry eposides in the LB.

The decrease in runoff from ~10.8 (especially after 10.2 cal ky BP) to 9.7–9.6 cal ky BP (subunits 1E and 1F; Figs. 3 and 4h) was probably related to a moderate regional decline in precipitation in southern Iberia. This agrees with the decrease in deciduous *Quercus* and Mediterranean tree taxa observed in the MD95-2042 record (southwestern Iberia) (Chabaud et al., 2014) and in Mediterranean forest taxa in the Padul-15–05 record (southeastern Iberia) (Ramos-Román et al., 2018b) (Fig. 4b, 4c, 4d, and 4 h). Jalut et al. (2000) also identified an aridification pulse in the western Mediterranean basin during this specific period based on the pollen ratios between deciduous broad-leaf *vs* evergreen sclerophyllous trees. In any case, the environment in the LB area should have been moderately wet when the Early Holocene siliciclastic drop occurred (from ~10.7–10.2 to 9.7–9.6 cal ky BP; subunits 1E and 1F), since it was coeval with a carbonate content increase (+15%) without significant sulphate precipitation (Figs. 3, 4f, 4 h and 4i), indicating that the groundwater contribution, whose source water is ultimately precipitation in the recharge area, was still significant. The presence of aragonite would also suggest the presence of fresh surface water inputs (Höbig et al., 2016). Additionally, the significant accumulation of terrestrial organic matter (higher %TOC and C/N increase and fluctuating between 14 and 15) would support the hypothesis that, although runoff was reduced during this period, rainfall/humidity should have been high enough to promote the accumulation of some terrestrial organic matter from the catchment basin between ~10.2 and 9.6 cal ky BP (subunit 1F; Fig. 3).

A maximum in humidity in the western Mediterranean region was registered from ~9.5 to 7.5 cal ky BP (Dormoy et al., 2009; Anderson et al., 2011; Fletcher et al., 2012; Jiménez-Moreno and Anderson, 2012; Ramos-Román et al., 2018b), when rainfall was also significantly influenced by local Mediterranean moisture sources, especially during late winter-early spring (García-Alix et al., 2021). This period is coeval with other significant episodes of LB siliciclastic deposits in the Early-Middle Holocene transition (subunits 1G and 2A; Figs. 3 and 4h), interpreted as a runoff enhancement.

The humid environmental conditions observed in LB record during the Early Holocene would also agree with a nearby record from the Guadiana Valley (CM5) (southwestern Iberia), showing an increase in humidity conditions from ~11.8 to 11.2 cal ky BP, dry climate from ~11.2 to 9.1 cal ky BP and moist oceanic climate conditions from ~9.1 to 7.9 cal ky BP (Fletcher et al., 2007).

The LB record seems to be insensitive to the "8.2 ka cooling event" (Figs. 3, 4f, 4 g, 4 h and 4i), despite the marked environmental changes observed in the Atlantic tropics and northern and central Europe related to this event (e.g., Matero et al., 2017). A similar muted response to this event has been observed in other Mediterranean records that showed major environmental changes between 7.8 and 7.3 cal ky BP instead (e.g., Frisia et al., 2006; Dormoy et al., 2009b; Fletcher et al., 2010; Ramos-Román et al., 2018b).

4.3.2. Middle Holocene

The high humidity conditions recorded in LB started to decrease after ~7.8 cal ky BP, especially after ~7.3 cal ky BP, giving rise to an abrupt reduction in the siliciclastic inputs into the lake (subunit 2B onwards; Figs. 3 and 4h). Regional records of the western Mediterranean showed a decrease in humid taxa such as deciduous *Quercus* and other Mediterranean forest taxa after this time, suggesting moisture all around the year and less winter precipitation (Chabaud et al., 2014). Although generally warm and humid conditions were recorded in southern Iberia between ~10.0 and 6.5–5.5 cal ky BP (Santos et al., 2003; Anderson

et al., 2011; Fletcher et al., 2012), other records in southeastern Iberia have shown a transitional period between ~7.0 and 5.0 cal yr BP, when climate evolved from a very humid Early Holocene to a dry Late Holocene (Rodrigo-Gámiz et al., 2011; Jiménez-Moreno and Anderson, 2012; García-Alix et al., 2012; Jiménez-Espejo et al., 2014; Ramos-Román et al., 2018b, among others). This transitional period showed no important siliciclastic inputs from the catchment basin in the LB, but the atomic C/N ratio exhibited the highest (but oscillating) values in the record (subunits 2B and 2C; Fig. 4g and 4 h). Although these are compatible with a mixed contribution from both algal and terrestrial organic matter, they point towards a much more organic contribution from the catchment basin (slight runoff) than in rest of the record. The C/N ratio started to decrease after ~4.8 cal ky BP, which agrees with an enhancement of arid conditions after ~4.6 cal ky BP in the neighboring Guadalquivir marshland area in southwestern Iberia (Jiménez-Moreno et al., 2015) (Fig. 4e and 4 g). The LB also registered this aridification trend and the sulphate and dolomite content started to gradually increase after 4.4 cal ky BP until 3.5 cal ky BP, and more significantly after this date (subunit 2D onwards; Fig. 3a and 4i). The magnitude of the occasional sulphate increase at 4.4 cal ky BP deduced by XRD analyses is much higher than the sulphate content variation obtained from XRF core scanner data (Fig. 3). Carbonate content, estimated by both decarbonation and XRD techniques, show a similar abrupt and occasional decrease at this age, coeval with an abrupt %TOC rise (Fig. 3). %TOC reached the highest values in the record at ~4.4 cal ky BP suggesting a large accumulation of organic matter with a likely algal origin, according to the C/N atomic ratio (Figs. 3 and 4g). These abrupt and occasional changes could be linked with the called 4.2 ka BP worldwide climatic event that has been registered in many Mediterranean records as short and intense arid episodes from 4.4 to 4.1 cal ky BP (Bini et al., 2019).

4.3.3. Late Holocene

The significant sulphate increase after 3.5 cal ky BP (subunit 2D) exhibited an inverse relationship with both the siliciclastic and the carbonate content (Fig. 4f, 4 h and 4i), suggesting high evaporation in the lake water, which at certain times could have also been triggered summer desiccation in the wetland. This change at 3.5 cal ky BP towards drier conditions coincided with an interval of rapid climate change observed worldwide between 3.5 and 2.5 cal ky BP and associated with a high-latitude cooling and low-latitude aridity (Mayewski et al., 2004). Slightly more humid conditions occurred from 2.4 to 1.7 cal ky BP in the LB record coinciding with the Iberian Roman Humid Period (IRHP), deduced by a slight decrease in the sulphate content coeval with a slowdown in the siliciclastic decrease (Fig. 4h and 4i). The sedimentary record of the Zóñar Lake, also in the Guadalquivir River Basin, displayed a similar pattern during the IRHP, registering more runoff (detrital) inputs and a reduction of the gypsum formation (Martín-Puertas et al., 2009b). In any case, the high sulphate content of the LB record during this period point towards overall dry conditions in the LB wetland.

Although the first evidences of intense anthropogenic environmental alterations in southern Iberia dated back to the Copper/Bronze Ages, when forest suffered major retractions (Carrión et al., 2007), human activities became more common since the Iberian/Roman periods (Martín-Puertas et al., 2009b; García-Alix et al., 2013), being southern Iberia one of the areas more affected by Roman mining activities in Europe (Kern et al., 2021). In this respect, different human activities such as livestock, lake draining for agriculture, or mining could have affected the environments in the LB and surroundings, and their signals could have been recorded in the LB sedimentary record. Heavy metal pollution, caused by human-induced accumulations of Pb, Cu, Zn, or As, for example, is one of the evidences of anthropogenic impact on historical sedimentary records in southern Spain, such as in the estuarine area of the Guadalquivir Valley (Nocete et al., 2005), Zoñar Lake (Martín-Puertas et al., 2010), or the alpine Laguna de Río Seco (García-Alix et al., 2013). Close archaeological sites to LB in the Guadalquivir Basin have registered heavy metal pollution related to metallurgy development since the Third millennium BCE (Nocete et al., 2005). Nevertheless, the inorganic geochemical analyses performed in the sedimentary record of the LB have not revealed any kind of human-related heavy metal pollution indicators (i.e., abnormal enrichments of heavy metals that are not common in the study area) that could have been brought into the lake by runoff in periods of enhanced development of mining and metallurgy activities in southern Iberian such as the Metal Ages or the Roman Times.

The decreasing trend in the C/N atomic ratio that started in the Middle Holocene depicted a sharp C/N increase (from 4.1 to 9 values) after ~0.4 cal ky BP (Fig. 4g). This was likely caused by some occasional inputs of terrestrial organic matter from the catchment that could probably be related to cultivation of cereal and other crops and soil erosion, although this interpretation has not been confirmed by siliciclastic inputs. Apart from this evidence, our Late Holocene record of the LB does not exhibit any other clear evidence of human impacts that could have affected the environmental features of the basin before the 20th century. This contrasts with the neighboring Zóñar Lake record, which was anthropically affected when southern Iberia was part of the Roman Empire (Martín-Puertas et al., 2009b). During Roman times, the area of the La Lantejuela complex was part of the territory of two Roman towns Astigi and Urso; more specifically, the LB basin was part of the Urso territory and a small settlement was established nearby (Castro García, 2019). Nevertheless, it seems that human activities in Roman times did not disturb significantly the natural ecosystem of LB since there is a lack of any apparent evidence of human activities in the lithological and geochemical record of LB. Conversely, the LB record during this period registered a slight increase in the humid conditions (Fig. 4f, 4 h and 4i) as it has been observed in other paleoenvironmental records in southern Iberia as a response to more precipitation, and probably the predominance of a negative North Atlantic Oscillation mode during the Iberian-Roman Humid Period (Martín-Puertas et al., 2009a; Ramos-Román et al., 2016; 2018a; López-Avilés et al., 2021).

4.3.4. Last century

The LB is one of the two best preserved wetlands in La Lantejula playa-lake complex, since the other wetlands were drained and transformed into crop fields in two stages: the end of the 19th century (Laguna Ruiz-Sánchez playa-lake, see LRS in Fig. 6a) and the second half of the 20th century (the rest of the playa-lakes). The LB and LCC playa-lakes remained almost unaltered until the end of the 20th century, when this area was declared Natural Reserve (Rodríguez-Rodríguez, 2007; Rodríguez-Rodríguez et al., 2008; Fajardo de la Fuente, 2018) (Figs. 1 and 6). Therefore, the most important human impacts on this playa-lake complex are related to local strategies of water management and land use change to avoid flooding and extracting groundwater for agricultural purposes; (Rodríguez-Rodríguez, 2007; Rodríguez-Rodríguez et al., 2008; Beltran et al., 2012). Previous studies based on the hydrogeology and hydrochemistry in this area (Rodríguez-Rodríguez, 2007; Rodríguez-Rodríguez et al., 2008; Beltran et al., 2012), suggest that the hydrological features of the LB playa-lake have not been anthropically altered in recent times except for the hydroperiod. The LB receives water from the O-LL aquifer when the piezometric level in the area is high, but the water level in the lake drops when the piezometric level decreases during the warm and dry summer season, which is amplified by massive groundwater extractions for extensive farmer irrigation in this season (Beltran et al., 2012). This scenario along with the high evapotranspiration in the area during the warm and dry season (Rodríguez-Rodríguez et al., 2008) modifies the natural relationship between the LB wetland and the aquifer (Rodríguez-Rodríguez, 2007; Rodríguez-Rodríguez et al., 2008; Beltran et al., 2012) and favors the precipitation of evaporites, mostly gypsum.

Similarly, the studied proxies in the LB-15–01 record evidenced that it is in the ~20th century, especially in the second half, when sediment accumulation rates abruptly increased, the gypsum content reached the

maximum values in the record and subsequently decreased coeval with abrupt siliciclastic and TOC% increases (unit 3; Figs. 2, 3, 4h, 4i and S1). These sudden oscillations might well be related to the dual effect of both 1) changes in the land use (extensive agriculture) that gave rise to more erosion in the catchment basin and 2) intensive groundwater pumping, that favored the lake desiccation in the warm and dry season, and thus the evaporite precipitation. These two phenomena have been widely identified in the studied area as current ecological impacts on these vulnerable ecosystems (Beltran et al., 2012). This agrees regionally with the neighboring Zóñar Lake, which also registered an important human impact in the last 50 years with more siliciclastic contribution from the catchment related to changes in the land use (Martín-Puertas et al., 2009b).

5. Conclusions

The sedimentary record of the Laguna de la Ballestera playa-lake, located in the La Lantejuela playa-lake complex, registered the response of the local environments to the climatic evolution of the western Mediterranean since the YD-Early Holocene transition, and only in the 20th century depicted potential clear evidences of human impacts.

The highest lake level and maximum lake surface (high piezometry in the basin) were registered in the humid Early Holocene, probably related to major surface water contribution from the Peinado-Salado catchment (low salinity). This surface water contribution along with the high piezometric levels gave rise to a flooded La Lantejuela basin during the most humid stages (Fig. 5a and b). The Middle Holocene was a transitional period, which agrees with other paleoenvironmental records from the western Mediterranean region, and surface water inputs and groundwater discharge were balanced in the LB system, registering medium salinity and piezometric levels. In this scenario the lake level and lake surface decreased (Fig. 5c). The final stages of the system are recorded during the arid Late Holocene, when runoff abruptly decreased giving rise to a negative balance between water inputs and outputs, and eventually, the current playa-lake system developed. In this stage, direct precipitation and groundwater discharge would have been the main water inputs and direct evapotranspiration the main water output. As a result, density-driven groundwater brine below the playa floor prevented lake recharge, and thus, groundwater discharge only entered in the playa through the shore, after rainy periods when the piezometric level rose (same hydrogeological setting as for Zarracatín, Gosque and Fuente de Piedra playa-lakes (Kohfahl et al., 2008) (Fig. 5d). The precipitation of gypsum, salts and dolomite was then significant. This situation was even more extreme in the latest Holocene, when enhanced summer desiccation affected the LB playa-lake, giving rise to the highest precipitation of gypsum and salts in the record (Fig. 5e). Therefore, the environmental evolution of this area has only been partially disturbed by anthropogenic forcing in recent times. An attempt of natural restoration of the whole La Lantejuela complex could be done if integrated water management and planning strategies were established in the area and the Laguna de la Ballestera wetland to recover its natural hydroperiod and reduce the evaporite precipitation.

Declaration of Competing Interest

The authors declare that they have no known competing financial interests or personal relationships that could have appeared to influence the work reported in this paper.

Acknowledgements

This study was supported by the action “Proyectos I + D + i del Programa Operativo FEDER 2018 - Junta de Andalucía-UGR” [grant number B-RNM-144-UGR], the Spanish Government (Ministerio de Economía y Competividad) and the European Regional Development Fund (ERDF - FEDER) [grant numbers CGL2013-47038-R and CGL2017-85415-R], and the Junta de Andalusia [grant numbers P18-RT-871 and Retos P20_00059, and research group RNM-190]. A.G.-A. was supported by a Ramón y Cajal Fellowship RYC of the Spanish Government (Ministerio de Economía y Competividad) [grant number 2015-18966]. A.L.-A PhD was funded by a fellowship of the Spanish Government (Ministerio de Economía y Competividad) [grant number BES-2018-084293]. F.G was financially supported by a Ramón y Cajal Fellowship (RYC2020-029811-I) of the Spanish Government (Ministerio de Economía y Competividad). The Open Access Publication Charge was funded by the University of Granada / CBUA.

Appendix A. Supplementary material

Supplementary data to this article can be found online at https://doi.org/10.1016/j.catena.2022.106292.

References

Anderson, R.S., Jiménez-Moreno, G., Carrión, J.S., Pérez-Martinez, C., 2011. Postglacial history of alpine vegetation, fire, and climate from Laguna de Río Seco, Sierra Nevada, southern Spain. Quat. Sci. Rev. 30, 1615–1629.

Bahr, A., Jiménez-Espejo, F.J., Kolasinac, N., Grunert, P., Hernández-Molina, F.J., Röhl, U., Voelker, A.H.L., Escutia, C., Stow, D.A.V., Hodell, D., Alvarez-Zarikian, C. A., 2014. Deciphering bottom current velocity and paleoclimate signals from contourite deposits in the Gulf of Cádiz during the last 140 kyr: An inorganic geochemical approach. Geochemistry. Geophys. Geosystems 15, 3145–3160.

Belmaker, R., Lazar, B., Stein, M., Taha, N., Bookman, R., 2019. Constraints on aragonite precipitation in the Dead Sea from geochemical measurements of flood plumes. Quat. Sci. Rev. 221, 105876.

Beltran, M., Moral, F., Rodríguez-Rodríguez, M., 2012. Changes in the hydrological functioning of a playa-lake complex under increasing agricultural pressures (Andalusia, Southern Spain). Water Environ. J. 26, 212–223.

Ben Dor, Y., Flax, T., Levitan, I., Enzel, Y., Brauer, A., Erel, Y., 2021. The paleohydrological implications of aragonite precipitation under contrasting climates in the endorheic Dead Sea and its precursors revealed by experimental investigations. Chem. Geol. 576, 120261.

Bini, M., Zanchetta, G., Perşoiu, A., Cartier, R., Català, A., Cacho, I., Dean, J.R., Di Rita, F., Drysdale, R.N., Finnè, M., Isola, I., Jalali, B., Lirer, F., Magri, D., Masi, A., Marks, L., Mercuri, A.M., Peyron, O., Sadori, L., Sicre, M.-A., Welc, F., Zielhofer, C., Brisset, E., 2019. The 4.2 ka BP Event in the Mediterranean region: an overview. Clim. Past 15, 555–577.

Blaauw, M., Christen, J.A., 2011. Flexible paleoclimate age-depth models using an autoregressive gamma process. Bayesian Anal. 6, 457–474.

Camuera, J., Jiménez-Moreno, G., Ramos-Román, M.J., García-Alix, A., Jiménez-Espejo, F.J., Toney, J.L., Anderson, R.S., 2021. Chronological control and centennial-scale climatic subdivisions of the Last Glacial Termination in the western Mediterranean region. Quat. Sci. Rev. 255, 106814.

Camuera, J., Jiménez-Moreno, G., Ramos-Román, M.J., García-Alix, A., Toney, J.L., Anderson, R.S.S., Jiménez-Espejo, F., Kaufman, D., Bright, J., Webster, C., Yanes, Y., Carrión, J.S., Ohkouchi, N., Suga, H., Yamame, M., Yokoyama, Y., Martínez-Ruiz, F., 2018. Orbital-scale environmental and climatic changes recorded in a new ~200,000-year-long multiproxy sedimentary record from Padul, southern Iberian Peninsula. Quat. Sci. Rev. 198, 91–114.

Camuera, J., Jiménez-Moreno, G., Ramos-Román, M.J.M.J., García-Alix, A., Toney, J.L.J. L., Anderson, R.S.S., Jiménez-Espejo, F., Bright, J., Webster, C., Yanes, Y., Carrión, J. S.J.S., 2019. Vegetation and climate changes during the last two glacial-interglacial cycles in the western Mediterranean: A new long pollen record from Padul (southern Iberian Peninsula). Quat. Sci. Rev. 205, 86–105.

Carrión, J.S., Fernández, S., Jiménez-Moreno, G., Fauquette, S., Gil-Romera, G., González-Sampériz, P., Finlayson, C., 2010. The historical origins of aridity and vegetation degradation in southeastern Spain. J. Arid Environ. 74, 731–736.

Carrión, J.S., Fuentes, N., González-Sampériz, P., Sánchez Quirante, L., Finlayson, J.C., Fernández, S., Andrade, A., 2007. Holocene environmental change in a montane region of southern Europe with a long history of human settlement. Quat. Sci. Rev. 26, 1455–1475.

Castro García, M. del M., 2019. La Lantejuela, un complejo endorreico entre dos colonias béticas: Astigi y Urso., in: Lagóstena Barrios, L. (Ed.), Economía de Los Humedales : Prácticas Sostenibles y Aprovechamientos Históricos. Universitat de Barcelona, Barcelona.

Chabaud, L., Sánchez Goñi, M.F., Desprat, S., Rossignol, L., 2014. Land–sea climatic variability in the eastern North Atlantic subtropical region over the last 14,200 years: Atmospheric and oceanic processes at different timescales. The Holocene 24, 787–797.

Deevey, E.S., Gross, M.S., Hutchinson, G.E., Kraybill, H.L., 1954. The natural C14 contents of materials from hard-water lakes. Proc. Natl. Acad. Sci. 40, 285–288.

Dormoy, I., Peyron, O., Combourieu Nebout, N., Goring, S., Kotthoff, U., Magny, M., Pross, J., 2009. Terrestrial climate variability and seasonality changes in the Mediterranean region between 15 000 and 4000 years BP deduced from marine pollen records. Clim. Past 5, 615–632.

Fajardo de la Fuente, A., 2018. Ocaso y resurrección de los Humedales del complejo endorreico de las llanuras esteparias sevillanas. Écija y Osuna: Tierra de lagunas. Cuad. los Amigos los Museos Osuna 20, 164–174.
Fletcher, W.J., Boski, T., Moura, D., 2007. Palynological evidence for environmental and climatic change in the lower Guadiana valley, Portugal, during the last 13 000 years. The Holocene 17, 481–494.
Fletcher, W.J., Debret, M., Goñi, M.F.S., 2013. Mid-Holocene emergence of a low-frequency millennial oscillation in western Mediterranean climate: Implications for past dynamics of the North Atlantic atmospheric westerlies. The Holocene 23, 153–166.
Fletcher, W.J., Debret, M., Goñi, M.F.S., Sanchez Goñi, M.F., Goñi, M.F.S., 2012. Mid-Holocene emergence of a low-frequency millennial oscillation in western Mediterranean climate: Implications for past dynamics of the North Atlantic atmospheric westerlies. The Holocene 23, 153–166.
Fletcher, W.J., Goni, M.F.S., Peyron, O., Dormoy, I., 2010. Abrupt climate changes of the last deglaciation detected in a Western Mediterranean forest record. Clim. Past 6, 245–264.
Fletcher, W.J., Sánchez Goñi, M.F., 2008. Orbital- and sub-orbital-scale climate impacts on vegetation of the western Mediterranean basin over the last 48,000 yr. Quat. Res. 70, 451–464.
Fowler, A.J., Gillespie, R., Hedges, R.E.M., 1986. Radiocarbon Dating of Sediments. Radiocarbon 28, 441–450.
Frisia, S., Borsato, A., Mangini, A., Spötl, C., Madonia, G., Sauro, U., 2006. Holocene climate variability in Sicily from a discontinuous stalagmite record and the Mesolithic to Neolithic transition. Quat. Res. 66, 388–400.
García-Alix, A., Camuera, J., Ramos-Román, M.J., Toney, J.L., Sachse, D., Schefuß, E., Jiménez-Moreno, G., Jiménez-Espejo, F.J., López-Avilés, A., Anderson, R.S., Yanes, Y., 2021. Paleohydrological dynamics in the Western Mediterranean during the last glacial cycle. Glob. Planet. Change 202, 103527.
García-Alix, A., Jiménez-Espejo, F.J., Toney, J.L., Jiménez-Moreno, G., Ramos-Román, M.J., Anderson, R.S.S., Ruano, P., Queralt, I., Delgado Huertas, A., Kuroda, J., 2017. Alpine bogs of southern Spain show human-induced environmental change superimposed on long-term natural variations. Sci. Rep. 7, 7439.
García-Alix, A., Jimenez-Espejo, F.J.J., Lozano, J.A.A., Jiménez-Moreno, G., Martinez-Ruiz, F., García Sanjuán, L., Aranda Jiménez, G., García Alfonso, E., Ruiz-Puertas, G., Anderson, R.S.S., 2013. Anthropogenic impact and lead pollution throughout the Holocene in Southern Iberia. Sci. Total Environ. 449, 451–460.
García-Alix, A., Jiménez-Moreno, G., Anderson, R.S., Jiménez Espejo, F.J., Delgado Huertas, A., 2012. Holocene environmental change in southern Spain deduced from the isotopic record of a high-elevation wetland in Sierra Nevada. J. Paleolimnol. 48, 471–484.
Gimeno, L., Nieto, R., Trigo, R.M., Vicente-Serrano, S.M., López-Moreno, J.I., 2010. Where Does the Iberian Peninsula Moisture Come From? An Answer Based on a Lagrangian Approach. J. Hydrometeorol. 11, 421–436.
Höbig, N., Mediavilla, R., Gibert, L., Santisteban, J.I., Cendón, D.I., Ibáñez, J., Reicherter, K., 2016. Palaeohydrological evolution and implications for palaeoclimate since the Late Glacial at Laguna de Fuente de Piedra, southern Spain. Quat. Int. 407, 29–46.
Hurrell, J.W., Kushnir, Y., Ottersen, G., Visbeck, M., 2013. An Overview of the North Atlantic Oscillation. In: The North Atlantic Oscillation: Climatic Significance and Environmental Impact. American Geophysical Union, pp. 1–35.
IPCC, 2019. Climate Change and Land: an IPCC special report on climate change, desertification, land degradation, sustainable land management, food security, and greenhouse gas fluxes in terrestrial ecosystems. Geneve.
Jalut, G., Dedoubat, J.J., Fontugne, M., Otto, T., 2009. Holocene circum-Mediterranean vegetation changes: Climate forcing and human impact. Quat. Int. 200, 4–18.
Jalut, G., Esteban Amat, A., Bonnet, L., Gauquelin, T., Fontugne, M., 2000. Holocene climatic changes in the Western Mediterranean, from south-east France to south-east Spain. Palaeogeogr. Palaeoclimatol. Palaeoecol. 160, 255–290.
Jiménez-Espejo, F.J., García-Alix, A., Jiménez-Moreno, G., Rodrigo-Gámiz, M., Anderson, R.S., Rodríguez-Tovar, F.J., Martínez-Ruiz, F., Giralt, S., Delgado Huertas, A., Pardo-Igúzquiza, E., 2014. Saharan aeolian input and effective humidity variations over western Europe during the Holocene from a high altitude record. Chem. Geol. 374–375, 1–12.
Jiménez-Moreno, G., Anderson, R.S., 2012. Holocene vegetation and climate change recorded in alpine bog sediments from the Borreguiles de la Virgen, Sierra Nevada, southern Spain. Quat. Res. 77, 44–53.
Jiménez-Moreno, G., Rodríguez-Ramírez, A., Pérez-Asensio, J.N., Carrión, J.S., López-Sáez, J.A., Villarías-Robles, J.J.R., Celestino-Pérez, S., Cerrillo-Cuenca, E., León, Á., Contreras, C., 2015. Impact of late-Holocene aridification trend, climate variability and geodynamic control on the environment from a coastal area in SW Spain. The Holocene 25, 607–617.
Kern, O.A., Koutsodendris, A., Süfke, F., Gutjahr, M., Mächtle, B., Pross, J., 2021. Persistent, multi-sourced lead contamination in Central Europe since the Bronze Age recorded in the Füramoos peat bog. Germany. Anthropocene 36, 100310.
Ketterer, M.E., Hafer, K.M., Jones, V.J., Appleby, P.G., 2004. Rapid dating of recent sediments in Loch Ness: inductively coupled plasma mass spectrometric measurements of global fallout plutonium. Sci. Total Environ. 322, 221–229.
Klinge, M., Lehmkuhl, F., Schulte, P., Hülle, D., Nottebaum, V., 2017. Implications of (reworked) aeolian sediments and paleosols for Holocene environmental change in Western Mongolia. Geomorphology 292, 59–71.
Kohfahl, C., Rodriguez, M., Fenk, C., Menz, C., Benavente, J., Hubberten, H., Meyer, H., Paul, L., Knappe, A., López-Geta, J.A., Pekdeger, A., 2008. Characterising flow regime and interrelation between surface-water and ground-water in the Fuente de Piedra salt lake basin by means of stable isotopes, hydrogeochemical and hydraulic data. J. Hydrol. 351, 170–187.
Lang, N., Wolff, E.W., 2011. Interglacial and glacial variability from the last 800 ka in marine, ice and terrestrial archives. Clim. Past 7, 361–380.
Laskar, J., Robutel, P., Joutel, F., Gastineau, M., Correia, A.C.M., Levrard, B., 2004. A long-term numerical solution for the insolation quantities of the Earth. Astron. Astrophys. 428, 261–285.
Lionello, P., Malanotte-Rizzoli, P., Boscolo, R., Alpert, P., Artale, V., Li, L., Luterbacher, J., May, W., Trigo, R., Tsimplis, M., Ulbrich, U., Xoplaki, E., 2006. The Mediterranean climate: An overview of the main characteristics and issues. Dev. Earth Environ. Sci.
López-Avilés, A., García-Alix, A., Jiménez-Moreno, G., Anderson, R.S., Toney, J.L., Mesa-Fernández, J.M., Jiménez-Espejo, F.J., 2021. Latest Holocene paleoenvironmental and paleoclimate reconstruction from an alpine bog in the Western Mediterranean region: The Borreguil de los Lavaderos de la Reina record (Sierra Nevada). Palaeogeogr. Palaeoclimatol. Palaeoecol. 573, 110434.
López-Avilés, A., Jiménez-Moreno, G., García-Alix, A., García-García, F., Camuera, J., Scott Anderson, R., Sanjurjo-Sánchez, J., Arce Chamorro, C., Carrión, J.S., 2022. Post-glacial evolution of alpine environments in the western Mediterranean region: The Laguna Seca record. CATENA 211, 106033.
López-Sáez, J.A., Pérez-Díaz, S., Rodríguez-Ramírez, A., Blanco-González, A., Villarías-Robles, J.J.R., Luelmo-Lautenschlaeger, R., Jiménez-Moreno, G., Celestino-Pérez, S., Cerrillo-Cuenca, E., Pérez-Asensio, J.N., León, Á., 2018. Mid-late Holocene environmental and cultural dynamics at the south-west tip of Europe (Doñana National Park, SW Iberia, Spain). J. Archaeol. Sci. Reports 22, 58–78.
Manzano, S., Carrión, J.S., García-Murillo, P., López-Merino, L., 2019a. When dynamism is the baseline: long-term ecology of a Mediterranean seasonal wetland in the Doñana National Park (Southwestern Europe). Biodivers. Conserv. 28, 501–522.
Manzano, S., Carrión, J.S., López-Merino, L., Jiménez-Moreno, G., Toney, J.L., Amstrong, H., Anderson, R.S., García-Alix, A., Pérez, J.L.G., Sánchez-Mata, D., 2019b. A palaeoecological approach to understanding the past and present of Sierra Nevada, a Southwestern European biodiversity hotspot. Glob. Planet. Change 175, 238–250.
Manzano, S., Carrión, J.S., López-Merino, L., Ochando, J., Munuera, M., Fernández, S., González-Sampériz, P., 2018. Early to mid-Holocene spatiotemporal vegetation changes and tsunami impact in a paradigmatic coastal transitional system (Doñana National Park, southwestern Europe). Glob. Planet. Change 161, 66–81.
Maréchal, B., Prosperi, P., Rusco, E., 2008. Implications of soil threats on agricultural areas in Europe. In: Toth, G., Montanarella, L., Rusco, E. (Eds.), Threats to Soil Quality in Europe EUR 23438 EN. Office for Official Publications of the European Communities, Luxembourg, pp. 129–138.
Martín-Puertas, C., Jiménez-Espejo, F., Martínez-Ruiz, F., Nieto-Moreno, V., Rodrigo, M., Mata, M.P., Valero-Garcés, B.L., 2010. Late Holocene climate variability in the southwestern Mediterranean region: an integrated marine and terrestrial geochemical approach. Clim. Past Discuss. 6, 1655–1683.
Martín-Puertas, C., Valero-Garcés, B.L., Brauer, A., Mata, M.P., Delgado-Huertas, A., Dulski, P., 2009a. The Iberian-Roman Humid Period (2600–1600 cal yr BP) in the Zoñar Lake varve record (Andalucía, southern Spain). Quat. Res. 71, 108–120.
Martín-Puertas, C., Valero-Garcés, B.L., Mata, M.P., Moreno, A., Giralt, S., Martínez-Ruiz, F., Jiménez-Espejo, F., 2009b. Geochemical processes in a Mediterranean Lake: a high-resolution study of the last 4,000 years in Zoñar Lake, southern Spain. J. Paleolimnol. 46, 405–421.
Martinez-Ruiz, F., Kastner, M., Gallego-Torres, D., Rodrigo-Gámiz, M., Nieto-Moreno, V., Ortega-Huertas, M., 2015. Paleoclimate and paleoceanography over the past 20,000 yr in the Mediterranean Sea Basins as indicated by sediment elemental proxies. Quat. Sci. Rev. 107, 25–46.
Martrat, B., Grimalt, J.O., Lopez-Martinez, C., Cacho, I., Sierro, F.J., Flores, J.A., Zahn, R., Canals, M., Curtis, J.H., Hodell, D.A., 2004. Abrupt Temperature Changes in the Western Mediterranean over the past 250,000 Years. Science 306, 1762–1765.
Martrat, B., Grimalt, J.O., Shackleton, N.J., Abreu Lucia de, Hutterli, M.A., Stocker, T.F., 2007. Four Climate Cycles of Recurring Deep and Surface Water Destabilizations on the Iberian Margin. Science 317, 502-417.
Matero, I.S.O., Gregoire, L.J., Ivanovic, R.F., Tindall, J.C., Haywood, A.M., 2017. The 8.2 ka cooling event caused by Laurentide ice saddle collapse. Earth Planet. Sci. Lett. 473, 205–214.
Mayewski, P.A., Rohling, E.E., Curt Stager, J., Karlén, W., Maasch, K.A., Meeker, L.D., Meyerson, E.A., Gasse, F., van Kreveld, S., Holmgren, K., Lee-Thorp, J., Rosqvist, G., Rack, F., Staubwasser, M., Schneider, R.R., Steig, E.J., 2004. Holocene climate variability. Quat. Res. 62, 243–255.
McFadden, L.D., McAuliffe, J.R., 1997. Lithologically influenced geomorphic responses to Holocene climatic changes in the Southern Colorado Plateau, Arizona: A soil-geomorphic and ecologic perspective. Geomorphology 19, 303–332.
Mediavilla, R., Santisteban, J.I., López-Cilla, I., Galán de Frutos, L., de la Hera-Portillo, Á., 2020. Climate-Dependent Groundwater Discharge on Semi-Arid Inland Ephemeral Wetlands: Lessons from Holocene Sediments of Lagunas Reales in Central Spain. Water 12, 1911.
Meyers, P.A., 2003. Applications of organic geochemistry to paleolimnological reconstructions: a summary of examples from the Laurentian Great Lakes. Org. Geochem. 34, 261–289.
Montes, C., Gonzalez-Capitel, E., Molina, F., Moreira, J.M., Rubio, J.C., Rodriguez, M., Gonzalez, C., Rodriguez, I., 2004. Plan Andaluz de Humedales (Andalusian Wetland Plan). Andalusian Ministry of Environment, Seville, Spain.
Moral Martos, F., 2016. Caracterización y origen de las lunetas asociadas a las lagunas de La Lantejuela (Sevilla, España). Geogaceta 59, 3–6.
Moreira Madueño, J.M., 2005. Caracterización Ambiental de Humedales de Andalucía. Junta de Andalucía, Sevilla.
Moreno, A., Cacho, I., Canals, M., Grimalt, J.O., Sánchez-Goñi, M.F., Shackleton, N., Sierro, F.J., 2005. Links between marine and atmospheric processes oscillating on a

millennial time-scale. A multi-proxy study of the last 50,000yr from the Alboran Sea (Western Mediterranean Sea). Quat. Sci. Rev. 24, 1623–1636.
Nelson, D.W., Sommers, L.E., 1983. Total Carbon, Organic Carbon, and Organic Matter. Methods Soil Anal, Agronomy Monographs.
Nocete, F., Álex, E., Nieto, J.M., Sáez, R., Bayona, M.R., 2005. An archaeological approach to regional environmental pollution in the south-western Iberian Peninsula related to Third millennium BC mining and metallurgy. J. Archaeol. Sci. 32, 1566–1576.
Olsson, I., 1979. No Title, in: Radiocarbon Dating: Proceedings of the Ninth International Conference, Los Angeles and La Jolla, 1976. University of California Press, Berkeley, pp. 613–618.
Putz, H., Brandenburg, K., 2021. Match! - Phase Analysis using Powder Diffraction, Crystal Impact.
Ramos-Román, M.J., Jiménez-Moreno, G., Camuera, J., García-Alix, A., Anderson, R.S., Jiménez-Espejo, F.J., Carrión, J.S., 2018a. Holocene climate aridification trend and human impact interrupted by millennial- and centennial-scale climate fluctuations from a new sedimentary record from Padul (Sierra Nevada, southern Iberian Peninsula). Clim. Past 14, 117–137.
Ramos-Román, M.J., Jiménez-Moreno, G., Camuera, J., García-Alix, A., Scott Anderson, R., Jiménez-Espejo, F.J., Sachse, D., Toney, J.L., Carrión, J.S., Webster, C., Yanes, Y., 2018b. Millennial-scale cyclical environment and climate variability during the Holocene in the western Mediterranean region deduced from a new multi-proxy analysis from the Padul record (Sierra Nevada, Spain). Glob. Planet. Change 168, 35–53.
Ramos-Román, M.J., Jiménez-Moreno, G., Camuera, J., García-Alix, A., Scott Anderson, R., Jiménez-Espejo, F.J.F.J., Sachse, D., Toney, J.L., Carrión, J.S., Webster, C., Yanes, Y., 2018c. Millennial-scale cyclical environment and climate variability during the Holocene in the western Mediterranean region deduced from a new multiproxy analysis from the Padul record (Sierra Nevada, Spain). Glob. Planet. Change 168, 35–53.
Reimer, P.J., Austin, W.E.N., Bard, E., Bayliss, A., Blackwell, P.G., Bronk Ramsey, C., Butzin, M., Cheng, H., Edwards, R.L., Friedrich, M., Grootes, P.M., Guilderson, T.P., Hajdas, I., Heaton, T.J., Hogg, A.G., Hughen, K.A., Kromer, B., Manning, S.W., Muscheler, R., Palmer, J.G., Pearson, C., van der Plicht, J., Reimer, R.W., Richards, D.A., Scott, E.M., Southon, J.R., Turney, C.S.M., Wacker, L., Adolphi, F., Büntgen, U., Capano, M., Fahrni, S.M., Fogtmann-Schulz, A., Friedrich, R., Köhler, P., Kudsk, S., Miyake, F., Olsen, J., Reinig, F., Sakamoto, M., Sookdeo, A., Talamo, S., 2020. The IntCal20 Northern Hemisphere Radiocarbon Age Calibration Curve (0–55 cal kBP). Radiocarbon 62, 725–757.
Rodrigo-Gámiz, M., Martínez-Ruiz, F., Jiménez-Espejo, F.J., Gallego-Torres, D., Nieto-Moreno, V., Romero, O., Ariztegui, D., 2011. Impact of climate variability in the western Mediterranean during the last 20,000 years: oceanic and atmospheric responses. Quat. Sci. Rev. 30, 2018–2034.
Rodríguez-Rodríguez, M., 2007. Hydrogeology of ponds, pools, and playa-lakes of southern Spain. Wetlands 27, 819–830.
Rodríguez-Rodríguez, M., Moral, F., Benavente, J., 2008. Hydrogeological characteristics of a groundwater-dependent ecosystem (La Lantejuela, Spain). Water Environ. J. 22, 137–147.
Rodríguez-Rodríguez, M., Moral, F., Benavente, J., Beltrán, M., 2010. Developing hydrological indices in semi-arid playa-lakes by analyzing their main morphometric, climatic and hydrochemical characteristics. J. Arid Environ. 74, 1478–1486.
Rodriguez-Rodriguez, M., Schilling, M., 2014. A hydrological simulation of the water regime in two playa lakes located in southern Spain. J. Earth Syst. Sci. 123, 1295–1305.
Roeser, P., Franz, S.O., Litt, T., 2016. Aragonite and calcite preservation in sediments from Lake Iznik related to bottom lake oxygenation and water column depth. Sedimentology 63, 2253–2277.
Santos, L., Sánchez-Goñi, M., Freitas, M., 2003. No Title. In: Ruiz Zapata, B., Dorado, M., Valdeolmillos, A. (Eds.), Quaternary Climatic Changes and Environmental Crises in the Mediterranean Region. Universidad de Alcalá, Alcalá de Henares, pp. 175–179.
Schirrmacher, J., Andersen, N., Schneider, R.R., Weinelt, M., 2020. Fossil leaf wax hydrogen isotopes reveal variability of Atlantic and Mediterranean climate forcing on the southeast Iberian Peninsula between 6000 to 3000 cal. BP. PLoS One 15, e0243662.
Schoute, J.F.T., Griede, J.W., Roeleveld, W., Mook, W.G., 1981. Radiocarbon dating of vegetation horizons, illustrated by an example from the Holocene coastal plain in the northern Netherlands. Geol. en Mijnb. 60, 453–459.
Schröder, T., López-Sáez, J.A., van't Hoff, J., Reicherter, K., 2020. Unravelling the Holocene environmental history of south-western Iberia through a palynological study of Lake Medina sediments. The Holocene 30, 13–22.
Sierro, F.J., Hodell, D.A., Andersen, N., Azibeiro, L.A., Jimenez-Espejo, F.J., Bahr, A., Flores, J.A., Ausin, B., Rogerson, M., Lozano-Luz, R., Lebreiro, S.M., Hernandez-Molina, F.J., 2020. Mediterranean Overflow Over the Last 250 kyr: Freshwater Forcing From the Tropics to the Ice Sheets. Paleoceanogr. Paleoclimatology 35.
Sinha, R., Smykatz-Kloss, W., Stüben, D., Harrison, S.P., Berner, Z., Kramar, U., 2006. Late Quaternary palaeoclimatic reconstruction from the lacustrine sediments of the Sambhar playa core, Thar Desert margin. India. Palaeogeogr. Palaeoclimatol. Palaeoecol. 233, 252–270.
Spanish National Weather Agency - AEMet Open Data, 2021. AEMet Open Data.
Toney, J.L., García-Alix, A., Jiménez-Moreno, G., Anderson, R.S., Moossen, H., Seki, O., 2020. New insights into Holocene hydrology and temperature from lipid biomarkers in western Mediterranean alpine wetlands. Quat. Sci. Rev. 240, 106395.
Toth, G., Adhikari, K., Varallyay, G., Toth, T., Bodis, K., Stolbovoy, V., 2008. Updated map of salt affected soils in the European Union. In: Toth, G., Montanarella, L., Rusco, E. (Eds.), Threats to Soil Quality in Europe EUR 23438 EN. Office for Official Publications of the European Communities, Luxembourg, pp. 65–77.
Trigo, R., Xoplaki, E., Zorita, E., Luterbacher, J., Krichak, S.O., Alpert, P., Jacobeit, J., Sáenz, J., Fernández, J., González-Rouco, F., Garcia-Herrera, R., Rodo, X., Brunetti, M., Nanni, T., Maugeri, M., Türkeş, M., Gimeno, L., Ribera, P., Brunet, M., Trigo, I.F., Crepon, M., Mariotti, A., 2006. Chapter 3 Relations between variability in the Mediterranean region and mid-latitude variability, in: Lionello, P., Malanotte-Rizzoli, P., Boscolo, R. (Eds.), Developments in Earth and Environmental Sciences. Elsevier, pp. 179–226.
Valero-Garcés, B.L., Delgado Huertas, A., Navas, A., Machín, J., González Morales, M.R., Kelts, K., 2000a. Quaternary palaeohydrological evolution of a playa lake: Salada Mediana, central Ebro Basin, Spain. Sedimentology 47, 1135–1156.
Valero-Garcés, B.L., González-Sampériz, P., Delgado Huertas, A., Navas, A., Machín, J., Kelts, K., 2000b. Lateglacial and Late Holocene environmental and vegetational change in Salada Mediana, central Ebro Basin. Spain. Quat. Int. 73 (74), 29–46.
Walker, M.J.C., Berkelhammer, M., Björck, S., Cwynar, L.C., Fisher, D.A., Long, A.J., Lowe, J.J., Newnham, R.M., Rasmussen, S.O., Weiss, H., 2012. Formal subdivision of the Holocene Series/Epoch: a Discussion Paper by a Working Group of INTIMATE (Integration of ice-core, marine and terrestrial records) and the Subcommission on Quaternary Stratigraphy (International Commission on Stratigraphy). J. Quat. Sci. 27, 649–659.
Zielhofer, C., Fletcher, W.J., Mischke, S., De Batist, M., Campbell, J.F.E., Joannin, S., Tjallingii, R., El Hamouti, N., Junginger, A., Stele, A., Bussmann, J., Schneider, B., Lauer, T., Spitzer, K., Strupler, M., Brachert, T., Mikdad, A., 2017. Atlantic forcing of Western Mediterranean winter rain minima during the last 12,000 years. Quat. Sci. Rev. 157, 29–51.